NPS-57Nt74081

NAVAL POSTGRADUATE SCHOOL

Monterey, California

FLOW CHARACTERISTICS IN SOLID FUEL RAMJETS.

by

Joseph T. Phaneuf, Jr.
and
David W. Netzer

Interim Report (Period 1 December 1973 - 1 July 1974)

Approved for public release; distribution unlimited

Prepared for:
Naval Weapons Center
China Lake, California 93955

NAVAL POSTGRADUATE SCHOOL
Monterey, California

Rear Admiral Isham Linder
Superintendent

Jack R. Borsting
Provost

The work reported herein was supported by the Naval Weapons Center, China Lake, California.

This report was prepared by:

UNCLASSIFIED

SECURITY CLASSIFICATION OF THIS PAGE *(When Data Entered)*

REPORT DOCUMENTATION PAGE		READ INSTRUCTIONS BEFORE COMPLETING FORM
1. REPORT NUMBER NPS-57Nt74081	2. GOVT ACCESSION NO.	3. RECIPIENT'S CATALOG NUMBER
4. TITLE *(and Subtitle)* Flow Characteristics in Solid Fuel Ramjets		5. TYPE OF REPORT & PERIOD COVERED Interim Report 1 Dec 73 - 1 Jul 74
		6. PERFORMING ORG. REPORT NUMBER
7. AUTHOR(s) Joseph T. Phaneuf, Jr. and David W. Netzer		8. CONTRACT OR GRANT NUMBER(s)
9. PERFORMING ORGANIZATION NAME AND ADDRESS Naval Postgraduate School Monterey, California 93940		10. PROGRAM ELEMENT, PROJECT, TASK AREA & WORK UNIT NUMBERS 62753;F31-334-302 PO-3-0081
11. CONTROLLING OFFICE NAME AND ADDRESS Naval Weapons Center Code 4576 China Lake, California 93555		12. REPORT DATE July 1974
		13. NUMBER OF PAGES 57
14. MONITORING AGENCY NAME & ADDRESS *(if different from Controlling Office)*		15. SECURITY CLASS. *(of this report)* UNCLASSIFIED
		15a. DECLASSIFICATION/DOWNGRADING SCHEDULE

16. DISTRIBUTION STATEMENT *(of this Report)*

Approved for public release; distribution unlimited

17. DISTRIBUTION STATEMENT *(of the abstract entered in Block 20, if different from Report)*

18. SUPPLEMENTARY NOTES

19. KEY WORDS *(Continue on reverse side if necessary and identify by block number)*

Ramjets
Solid Fuel
Flow Characteristics

20. ABSTRACT *(Continue on reverse side if necessary and identify by block number)*

An experimental investigation of the internal ballistics of solid fuel ramjets was conducted in order to determine the effects of inlet step size, inlet velocity and wall blowing on flow characteristics behind a backward facing step inlet.

It was shown that the reattachment point (zone) moves toward the step inlet with wall mass addition at a constant inlet mass flux. For a given step inlet, however, the leading edge of the reattachment zone was

DD FORM 1 JAN 73 1473 EDITION OF 1 NOV 65 IS OBSOLETE
S/N 0102-014-6601 |

UNCLASSIFIED

SECURITY CLASSIFICATION OF THIS PAGE *(When Data Entered)*

stationary with variations in inlet velocity. A point where the wall temperature and centerline static pressure profiles leveled off simultaneously was defined as the end of the reattachment zone. This zone spread out (grew thicker) both with increasing inlet velocity for a given step size, and with increasing step height. Maximum wall temperatures occurred downstream of the reattachment zone.

TABLE OF CONTENTS

LIST OF FIGURES

LIST OF TABLES

I. INTRODUCTION

A research project is currently being conducted at the Naval Postgraduate School to develop a model for the internal ballistics of solid fuel ramjets. Such a model would provide the design engineer with a working tool that would permit performance parameters and operating characteristics to be predicted. The ultimate goals of this project are to develop an analytical model that can be used to predict fuel regression rate and blow-off limits and to experimentally determine the fuel regression rate as a function of operating and configuration variables. Very little experimental data exist that can be used in the determination of the adequacy of such an analytical model.

The means of flame stabilization in solid fuel ramjets was developed originally by the United Technology Center [Ref. 1]. They found that a rearward facing step at the grain inlet provided an adequate flame holder much the same as it does in dump combustors which use liquid fuels. With this step inlet employed, solid fuel ramjet combustors have two distinct combustion zones as shown in Figure 1. In the recirculation zone, products and reactants are mixed, and in the limiting case a well-stirred reactor may be approached. Downstream of the flow reattachment the boundary layer develops and the combustion may be similar to that in a hybrid rocket in which kinetic effects are dominant.

Abbott and Kline [Ref. 2], Krall and Sparrow [Ref. 3], Boaz and Netzer [Ref. 4], and others have investigated the turbulent flow over a backward facing step. Abbott and Kline found that the recirculation zone behind the backward facing step consisted of a complex pattern of two-dimensional and three-dimensional zones ending at an unsymmetric reattach-

ment point. Their investigation employed water flow through a two-dimensional planar channel. It was found that the location of the reattachment point was not influenced by varying either pipe Reynolds number or inlet turbulence intensity, but did move further downstream when the step height was increased.

Krall and Sparrow also used water flow in their investigation of the flow through an orifice in an electrically heated circular tube. In this heated wall, axisymmetric experiment. they found that the local heat transfer coefficients in the recirculation, reattachment, and redevelopment zones were several times larger than those for fully developed turbulent pipe flow. The maximum heat transfer coefficient occurred in the vicinity of the reattachment point. Their results were in good agreement with those of Abbott and Kline in that the location of the reattachment point was not affected by changes in Reynolds number. They also found that for small step heights, h, (weak separations or flat recirculation zones) the peak Nusselt number was a well-defined point, but for large step heights (strong separations or thick recirculation zones) the peak Nusselt number spread out into a broad zone. This transition from a well-defined point to a broad zone occurred between $h/D = 0.16$ and $h/D = 0.25$, where D is the pipe diameter. The peak Nusselt number was located between 1.25 and 2.5 pipe diameters downstream of the initial separation. They also found that increasing the step height moved the peak point slightly down stream.

The results of Boaz and Netzer were in general agreement with the results of the above mentioned experimental studies even though air was used as the fluid medium instead of water. Visualization was obtained in a cold air flow through a tube behind a step inlet by injecting a colored fluid

mixture at the base of the step. Turbulence in the recirculation zone caused the fluid mixture to be broken up into tiny droplets which collected on the tube walls. Within the region of recirculation, the droplets on the wall moved toward the step face. The droplets were stationary at the flow reattachment point and moved downstream aft of it. Thus, the flow reattachment points were visually measured for several step sizes and Reynolds number conditions. Boaz and Netzer reported that the reattachment point was axially symmetric for most Reynolds number flows. But at high Reynolds numbers, the reattachment point varied around the circumference of the tube, offering a possible explanation of the "spreading out" of the peak Nusselt number reported by Krall and Sparrow.

All of the above investigations considered solid wall geometry with no wall mass addition. Jones, et al [Ref. 5], considered the effects of wall blowing on the recirculation zone flow characteristics using a two-dimensional planar model with schlieren photography. Generally, Jones' data were in good agreement with the other mentioned investigators. He stated that the location of the reattachment point seemed very stable and unaffected by the wall blowing and/or inlet velocities from the qualitative measurements that could be taken from the schlieren photographs.

All of the above investigations were for non-reacting flow conditions. Tests are required for reacting and non-reacting flows in a solid fuel ramjet geometry in which flow characteristics (i.e., velocity, mass fraction distribution, turbulence intensity, wall temperature profiles, etc.) are measured. Reacting flow measurements are, admittedly, extremely difficult. Therefore, this research was concerned with non-reacting flow

in which experiments were conducted in a realistic geometry to simulate a solid fuel ramjet with wall blowing. Air was primarily used as the blowing gas. Helium was used as the blowing gas for the tests in which mass fraction was measured. Helium was used with some reservation, since in a solid fuel ramjet the molecular weight of the wall species can be expected to be somewhat higher than for air.

II. METHOD OF INVESTIGATION

Measurements were taken in non-reacting flows for a variety of conditions using a pressure-jacketed porous bronze tube as the solid fuel ramjet model. Nominal test conditions are listed in Table I. Iron-constantan thermocouples were mounted axially on the porous bronze tube for measurement of temperature profiles along the wall. Velocity measurements were taken utilizing a total pressure rake and a centerline mounted pitot-static probe. Additional wall temperature measurements were made using a solid stainless steel tube in place of the porous bronze tube.

One data set was taken to determine mass fraction profiles by using unheated helium for wall blowing.

All of the data taken were used to determine the location of the reattachment point (zone) and the characteristics of the flow field. The results were compared with the work of previous investigators and with the modified PISTEP II [References 8 and 9] finite-differencing computer solution for the non-reacting flow field, which is currently under development.

III. DESCRIPTION OF APPARATUS

A. THE BASIC SOLID FUEL RAMJET MODEL

A schematic of the ramjet is shown in Figure 2 and the assembled layout in the photographs of Figures 3, 4, and 5. It consisted of a stainless steel cylindrical jacket in which was axially mounted a 1.27-inch I.D porous bronze tube to simulate wall blowing from the solid fuel in the actual motor. When air was employed as the blowing gas, it was drawn off from the main air feed system and controlled by a pressure valve and a choked orifice.

The main air feed system was powered by a Pennsylvania air compressor that provided air up to pressures of 150 psia. This air was fed into an air reservoir which could be directly supplied to the ramjet by a manually operated gate valve. When heated inlet air was desired, a Polytherm air heater was used to provide non-vitiated hot air to 500°F.

The ramjet unit itself was axially mounted in the test cell immediately downstream of two pneumatically operated Jamesbury ball valves that either vented main air to the atmosphere or allowed the air to pass through the ramjet. A standard ASME orifice flow meter was used to measure the flow rate of the air to the motor. A manually operated gate valve between the orifice and the motor was used to provide the desired flow rate through the motor.

Line pressure and differential pressure across the ASME orifice were recorded on a Honeywell Model 2106 Visicorder. All twenty-six iron-constantan thermocouples attached to the porous bronze tube, and the iron-constantan thermocouples associated with the ASME orifice and with the

choked orifice for blowing-gas flow measurement, were recorded on two Leeds and Northrup multi-print Strip Chart Recorders.

B. FLOW MEASUREMENT WITHIN SIMULATED MOTOR

Two methods of flow measurement were utilized in the experiments: a total pressure rake, and a centerline pitot-static probe. In addition the apparatus was designed to allow the use of miniature hot wire anemometers.

1. Total Pressure Rake

A total pressure rake was designed to axially traverse the porous bronze tube during test runs. Figure 6 is a drawing of the rake installed in the ramjet model. Plastic tubing connected the rake directly to a DATEX SP-101A Pressure Scanner powered by an SRC power supply model 3564. The pressure scanner output was measured by a zero to 15 psig Statham transducer and read on a DIGITEC D. C. millivoltmeter. This setup allowed rapid readings of the seven total and two static pressure probes of the rake. The axially oriented support tube for the rake was scribed for easy determination of probe location when inside the porous bronze tube.

2. Centerline Pitot-Static Probe

A pitot-static probe was designed so that it would fit interchangeably with the total pressure rake. Similarly, it was connected to the pressure scanner for rapid readings utilizing the millivoltmeter.

3. Hot Wire Anemometers

The apparatus was designed to allow use of miniature Thermo-Systems Incorporated (TSI) hot wires for measurement of the intensity of turbulence.

However, no measurements have been made to date. The configuration of the hot wires in the ramjet model are shown in Figure 7. Figures 5 and 7 also show the hot wire traverse mechanism which was designed to determine the radial position of the hot wire inside the porous bronze tube. The hot wires are connected directly to the TSI electronic equipment. A CALICO Series 8300 digital multimeter and a true RMS meter are connected so that DC and RMS voltages can be read directly. Additionally, a TEKTRONIX dual beam oscilloscope model R5030 is connected for visual observations of the hot wire output during test runs. This portion of the investigation is currently being conducted.

C. WALL TEMPERATURE MEASUREMENT

Twenty-six iron-constantan thermocouples were spot welded on the outside wall of the porous bronze tube and the non-porous stainless steel tubes. They were located on an axial line at points from a distance of one inch from the inlet end at intervals of 0.2 inches. The wires were bundled and fed through a Swagelock fitting access port in the exhaust plate of the ramjet model and connected to two Leeds and Northrup multiprint Strip Chart Recorders. Figure 8 shows the schematic of the wire-to-tube connections.

D. MASS FRACTION ANALYSIS

Bottled helium was connected to the blowing gas inlet, instead of the compressor air supply, for this test. The pressure rake was used in conjunction with the pressure scanner as before. This time, however, the output of the scanner, instead of being connected to the transducer, was attached by plastic tubing to a gas sampling tank in which was placed a previously calibrated hot wire anemometer. A vacuum pump was employed

to evacuate the tank to a constant pressure of four psia. A choked orifice flow plate inserted in the plumbing to the gas sampling tank kept the mass flow rate approximately constant over the entire range of helium and air mass ratios. Changes in hot wire readings gave relative changes in composition of the entrained gas. The hot wire anemometer was connected to the TSI instrument which allowed direct reading of changes in gas composition through the use of the CALICO D. C. multimeter. A schematic of the mass fraction analysis apparatus is shown in Figure 9. Figure 10 is a picture of the assembled hardware.

IV. EXPERIMENTAL PROCEDURE

A. FLOW MEASUREMENTS

Prior to running all tests it was necessary to calibrate the flow measuring devices. The motor air flow rate was measured using an A.S.M.E. sharp-edged orifice. A Visicorder was used to record the line pressure, P_1, and the pressure differential, Δp, across the orifice. A ten-foot water manometer board was employed for calibrating the low ΔP settings, and a mercury manometer for the higher settings. A Heise gauge was used as a secondary standard for calibrating the line pressure, P_1. Air temperatures were measured with a thermocouple and were recorded on a strip chart. The strip chart was specially equipped for recording temperature and was checked for accuracy at both the boiling and freezing points of water.

Line pressure, differential pressure, and line temperature were critical in the accurate measurement of inlet mass flow. Reference 6 outlines in detail the procedures for calculation of mass flow rate across an A.S.M.E. orifice.

A sonic choked flow nozzle, [Ref. 7] was used for controlling and measuring the flow rate of the wall blowing gas. A perfect gas with constant specific heat was assumed to expand isentropically through the nozzle.

B. SUMMARY OF NOMINAL TEST CONDITIONS

Nominal test conditions are summarized in Table I.

TABLE I

NOMINAL TEST CONDITIONS

Air Mass Flow ($\dot{m}$, lbm/sec)	.05	.07	.10	.15
Air Mass Flux (G, lbm/in^2-sec)	.039	.055	.079	.118
Inlet Temperature (F)	55	200		
Inlet Diameter (in)	.500	.770		
Step (h/D)	.303	.195		
Blowing rate (%$\dot{m}$)	10	10	10	7.5

C. PROCEDURES FOR COLD INLET AIR TESTS

In the initial runs,flow velocities and temperature profiles were measured for three inlet mass flux conditions. Both wall blowing and non-blowing tests were conducted using the large step size inlet (h/D = .303). Alternating rake and centerline pitot probe traverses were made at one-inch intervals from the exhaust plane to the inlet face. Pressure scanner output voltages were displayed on a D. C. millivoltmeter and were recorded at each station along the traverse. The pressure scanner was calibrated before each set of tests using a mercury manometer. During all runs, main inlet air control parameters were monitored continuously to insure constant mass flux through the motor. Wall blowing mass flow could be initiated or terminated at will by using a hand operated ball valve in close proximity to the motor. During the runs, the strip chart recorders were operated to obtain the

wall temperature profiles.

D. PROCEDURES FOR HOT INLET AIR TESTS

In the tests conducted with hot inlet air, flow velocities and temperature profiles were measured for four inlet mass flux conditions both with and without wall blowing. These tests all used the small step size inlet (h/D = .195). The procedure for this set of runs remained the same as for the cold inlet tests.

E. REATTACHMENT ZONE MEASUREMENT

During the first 26 runs, it was discovered that the pressure rake outermost probes went through a "plus-zero" to a "minus-zero" zone at about the position where one would expect to find the reattachment point. The downstream edge was taken to be the point where the flow near the wall first moved entirely downstream and the upstream edge where it first moved entirely upstream. Sixteen additional runs were made with the pressure rake and centerline pitot-static probe, with the specific purpose of measuring this "zero-zone" for the four heated inlet mass flow conditions. Wall temperature profile data were also collected.

F. MASS FRACTION ANALYSIS

Once the hot wire was calibrated for measuring mass fractions, the procedure for taking the data was relatively simple. The total pressure rake was used in conjunction with the pressure scanner. The gas sampling tank was connected, instead of the usual pressure transducer, to the output side of the scanner. Thus, by keeping the gas sampler plenum chamber at

a constant four psia to insure sonic flow through the choked nozzle inlet orifice, it was a simple matter to scan the seven total pressure stations and read the D.C. multimeter for hot wire output voltages. These converted directly into percentages of blowing gas.

Only one actual run was accomplished in the test cell. The amount of bottled helium on hand, and the rate at which ten percent blowing helium depleted the supply, precluded further runs.

A special calibration device was designed for this test and is schematically shown in Figure 11. Figure 12 is a picture of the assembled components. Pure helium and air were fed under pressures up to 300 psig into separate holding tanks. From the holding tanks, proportionate parts of each gas were fed through a choked orifice into a mixing chamber, according to the percentage of helium desired. The known mixture mass flow leaving the mixing chamber was routed through the TSI calibration tunnel. A pressure tap on the tunnel wall was used to withdraw the gas sample. The gas mixture passed through the choked nozzle orifice at the inlet of the gas sampling tank, which was evacuated to a constant four psia. The hot wire output for various mass fractions of helium were then recorded.

The error estimation for this phase of the research warrants comment. The mass flow rate formula for isentropic flow through a choked convergent nozzle is a function of total pressure and temperature and the ratio of specific heats. In the calibration procedure, the total pressure and temperature were static conditions, giving a specific mass flow rate through the sampling plenum for each mixture ratio. When the sampling device was connected to the ramjet model, the total pressure was greater

than for the calibration because of the velocity head. Thus, for the same mixture ratio, the flow rate in the sampling plenum was higher. This could yield false percentages of helium. An error analysis was done for the case of two percent helium and indicated a 0.3 percent error. The effect would be much more dramatic if the ramjet flow velocity was increased. One possible method to correct this situation would be to cap off the gas sampling tank after drawing off a sample and then record the hot wire output. This would eliminate velocity effects and make the hot wire output dependent almost entirely on the thermal conductivity of the mixture.

V. RESULTS AND DISCUSSION

A. REATTACHMENT POINT

Much of the emphasis in this research study was placed on the determination of the location of the reattachment point for flow over a backward facing step at the inlet of a cylindrical tube with and without wall mass addition. Defining a Reynolds number based on the height of the backward facing step as

$$Re_s = \frac{\rho V h}{\mu}$$

where

ρ = fluid density (lbm/ft^3)

V = average velocity at the step inlet (ft/sec)

h = step height (ft)

μ = fluid viscosity (lbm/sec-ft)

it was found that the leading edge of the reattachment zone remained constant for a given step inlet height for most Reynolds numbers. As the step height increased, the leading edge of the reattachment zone moved further downstream. The range of step Reynolds numbers encountered in this study are summarized in Table II.

TABLE II

SUMMARY OF RANGE OF REYNOLDS NUMBERS (STEP)

h/D \ G $\left[\frac{\text{lbm}}{\text{in}^2\text{-sec}}\right]$	0.039	0.055	0.079	0.118
.303 (COLD)	107,300	141,700	231,800	-----
.195 (COLD)	-----	46,900	58,600	78,200
.195 (HOT)	23,100	35,500	44,100	82,200

The results of the cold inlet flow measurements (Figures 13, 14 and 15) that utilized the large step inlet (h/D = .303) generally were in agreement with the subsequent runs utilizing the small step inlet. The fact that the recirculation zone extended through six inches of the seven-inch porous bronze tube length did not allow any practical analysis of the redevelopment region. The centerline static pressure profiles and velocity profiles did, however, indicate that the reattachment point or zone was located between three and one-half and five inches from the step inlet. The axial location where the centerline static pressure leveled to ambient conditions was taken to be the end of the reattachment zone. Figure 25 is a drawing of the typical reattachment zone pattern found in these tests. Since these tests were run without an exit nozzle, the velocities attained with this inlet were excessive except at the very low flow rates. In these tests, inlet air temperature was less than

the blowing air temperature. The noticeable non-symmetry in nearly all of the velocity profiles may partially be explained by the difficulty encountered in maintaining the designed dimensions in the rake itself and the accuracy of keeping it precisely on the centerline of the bronze tube. The pressure rake data have been plotted on the graphs according to the design dimensions between total pressure probes. In addition, the large step inlet may induce non-axisymmetric flow within the tube.

The hot air inlet runs (Figures 16 through 23) were better able to provide information concerning the reattachment point. By reducing the step size to h/D = .195, the reattachment zone moved closer to the inlet. This was expected from the results of previous investigators [Refs. 2, 3 and 4], and provided a better means of interpreting the centerline static pressure profile as well as the more gradual development of the fully developed turbulent pipe flow through the core of the model. Figure 26 is a drawing of the typical reattachment zone pattern of these hot air inlet, small step tests. In almost all cases, the centerline static pressure and wall temperature profiles achieved a definite leveling off point together. This was interpreted to be the end of the reattachment zone, the point at which pure pipe flow begins with its associated boundary layer development. A significant result is evident from the "zero zone" measurement runs (see Figures 20 through 23, the results of which are also presented in Figures 16 through 19). There is an apparent difference in the beginning of the reattachment zone between tests with blowing and tests without. In all but one case, the "zero zone" moved about 0.3 inches toward the inlet when blowing was introduced with the small step size. This happened at all

mass flow rates tested except the highest, which showed a movement of about 0.2 inches toward the inlet with wall blowing. Interestingly, as inlet mass flux increased, the width of the "zero zone" decreased for both blowing and non-blowing tests. However, in both cases, the center of the "zero zone" remained fixed except for high Reynolds number where it moved slightly downstream. It is thought that the "zero zone" leading edge of the reattachment region can physically be described by the illustration in Figure 27. The reattachment zone spreads out downstream with increasing inlet mass flux but the upstream edge remains approximately fixed. It is thought that this spreading out of the reattachment zone possibly results from the increased turbulent transport across the shear line with increased Reynolds number. That increased mixing across the shear line may spread the reattachment zone is also evident by comparing Figures 15 and 18. The large h/D and its associated large step Reynolds numbers indicate a much more spread out reattachment zone than the small h/D.

In every case, the maximum wall temperature occurred somewhat further downstream of the apparent end of the reattachment zone as indicated by the simultaneous leveling off of the centerline static pressure and wall temperature profiles. The point of maximum wall temperature varied from about 0.5 inches downstream of the end of the reattachment zone at the lowest inlet mass flux to about 2.0 inches downstream at the highest inlet mass flux. This result indicates that the point of maximum heat transfer is not coincident with the zone of reattachment and also is dependent upon the inlet mass flux.

Figure 24 compares the data of this investigation with the data of previous investigators. The centers of the "zero zone" regions established

by the results shown in Figures 20 through 23 were the points plotted for the blowing and non-blowing cases with heated inlet air through the small step inlet. The extent of the spreading out of the "zero-zone is indicated by the short dashed lines in the figure. The points chosen for the large step inlet employed are best estimates from careful profile analysis of the graphs of Figures 13 through 15, and from comparison with the reattachment zone characteristics of the small step inlet profiles plotted on Figures 16 through 19. Although the evidence of this investigation indicated a reattachment "region" or "zone" is more descriptive (as indicated in Figure 26), the stagnation point ("zero-zone") as described in Figure 27 was plotted on the graph of Figure 24 to allow a more analogous comparison with the data of previous investigators.

The unsymmetric reattachment points reported by Abbott and Kline [Ref. 2] are shown. Their work utilizing a two-dimensional channel with water flow showed the flow reattaching at different locations on each side. They also reported a spreading out of the reattachment point with increased step height as indicated by the dashed lines in Figure 24.

Boaz and Netzer used the Krall and Sparrow [Ref. 3] data for the location of maximum heat transfer coefficient to locate the reattachment point. These data are plotted in Figure 24. The data of this investigation are above that of Krall and Sparrow. If peak wall temperature was used to locate the reattachment point in this investigation (as was equivalently done for the Krall and Sparrow data), the difference between the results would be even greater. A possible explanation for this significant difference could be the differences in experimental apparatus. With heated inlet air and a cold tube wall, a variable heat transfer occurs

along and toward the wall, as one would expect in solid fuel ramjet combustion. Krall and Sparrow had an electrically heated wall, which directed the heat flow from the wall. In addition, outside wall temperatures are reported in this study whereas Krall and Sparrow corrected their data to inside wall temperatures.

Some additional comments are necessary concerning the experiments conducted in this study. For the non-blowing tests the porous tube had a stagnant plenum surrounding it. This may complicate the temperature profile somewhat when compared with a solid tube wall. In addition, the apparatus used in this experiment provided wall mass addition with practically no pressure drop across the tube wall. Thus, an approximately constant pressure plenum was supplying wall mass addition into a tube in which the static pressure increased in the direction of flow. This experimental condition would cause non-uniform blowing with more mass addition in the recirculation region than downstream. This is not characteristic of the solid fuel ramjet where mass addition is less in the recirculation region. However, the temperature profiles with and without wall blowing are quite similar, indicating that the non-uniform wall blowing had only small effects. Future tests should perhaps be conducted with the plenum divided into segments in order to provide more realistic ramjet injection rates. An apparatus using this construction is currently being used at the United Technology Center.

The temperatures obtained for the non-blowing condition using the porous bronze tube may be questionable because of the possible interaction of the tube flow with the stagnant gas in the plenum chamber which surrounded the tube. For this reason, additional tests were conducted using solid stainless steel tubes in place of the porous bronze tube. The temperature

profiles obtained are presented in Figure 28. These "non-blowing" profiles are quite similar to those obtained with stagnant gas behind the porous bronze tube.

The Krall and Sparrow data indicate higher rates of heat transfer in the recirculation region than downstream of the reattachment zone, where the boundary layer develops. However, in the solid fuel ramjet in which chemical reactions occur, the fuel regression rate is a minimum near the inlet and increases to a maximum somewhere downstream or near the reattachment point. Interestingly, the temperature profiles obtained in this study follow closely the fuel regression profiles obtained in the solid fuel ramjet.

Jones, et al [Ref. 5], using schlieren photography analysis of air flow through a two-dimensional channel, experimented with wall blowing and found no measurable difference in reattachment point location between blowing and non-blowing conditions. The present investigation, however, showed that a small, but significant shift upstream occurred with wall blowing for a constant inlet mass flux.

The initial results of reattachment point dependence on step inlet size obtained using PISTEP II [Refs. 8 and 9], the computer solution model, are also plotted in Figure 24 for the no wall blowing condition. PISTEP II, like Jones' data, predicts little effect of blowing on the flow in the recirculation region and the reattachment point. The results of the initial PISTEP II calculation did, however, show that the reattachment point moves slightly toward the step inlet with wall blowing. Current work with PISTEP II in which more realistic boundary conditions are employed may indicate different results.

B. MASS FRACTION ANALYSIS

Due to the limited amount of data collected for this phase of the investigation, no definite conclusions were drawn. The mass fraction data are presented in Figure 29. It is interesting to note the unsymmetrical distribution of helium at the locations sampled. This is indicative of unsymmetrical air flow. The apparent centerline of the helium distribution is below that of the geometrical centerline of the tube.

In the lower half of the tube the high percentage of helium is at the wall and decreases radially to a constant value. Axially, the helium percentage increases with distance from the inlet.

In the upper half of the tube the radial distribution behaves in the same manner as the lower half. However, the helium content decreases and then increases in the axial direction.

An unsymmetrical as it may be, there seems to be a definite pattern to the helium distribution. Both the upper and lower distributions are indicative of wall species accumulating from boundary layer blowing and possibly from helium escaping the recirculation zone. Note that all stations sampled were downstream of the reattachment point where the boundary layer was developing.

VI. CONCLUSIONS

(1) The leading edge of the reattachment zone, idealized by a pseudo-stagnation point, is upstream of the point where wall temperature and centerline static pressure level off.

(2) The leading edge of the reattachment zone does not move with variations in inlet velocity but the zone itself spreads out with increasing inlet velocity.

(3) Wall blowing moves the leading edge of the reattachment zone upstream.

(4) Maximum wall temperature is located downstream of the reattachment zone and the wall temperature profile closely approximates the fuel regression profile in an actual solid fuel ramjet.

(5) With approximately 10% blowing helium, the mass fraction analysis showed the average helium close to the walls was about 12%, and around the centerline about 6%.

LIST OF REFERENCES

1. Iwanciow, B.L., Hulzman, A.L., Dunlap, R., "Combustion Stabilization in a Solid Fuel Ramjet," 10th JANNAF Combustion Meeting, CPIA Publication 243, Vol. III, pp. 197-214, December, 1973.

2. Abbott, D.E. and Kline, J. S., "Experimental Investigation of Subsonic Turbulent Flow Over Single and Double Backward Facing Steps," Journal of Basic Engineering, p. 317, September 1962.

3. Krall, K. M. and Sparrow, E. M., "Turbulent Heat Transfer in Separated, Reattached, and Redevelopment Regions of a Circular Tube," Journal of Heat Transfer, p. 131, February 1966.

4. Naval Postgraduate School Report 57NT73031A, An Investigation Of The Internal Ballistics Of Solid Fuel Ramjets, by L. D. Boaz and D. W. Netzer, 1 March 1973.

5. Naval Postgraduate School Report 57NT73091B, An Investigation Of The Internal Ballistics of Solid Fuel Ramjets - A Progress Report, by L. D. Boaz, C. E. Jones, III, and D. W. Netzer, September 1973.

6. Flow Measurement - Supplement to Power Test Codes, v. 19.5;4, The American Society of Mechanical Engineers, 1959.

7. John, James E. A., Gas Dynamics, p. 39-46, Allyn and Bacon, 1969.

8. Gosman, A. D., Pun, W. M., Runchal, A. K. Spalding, D. B., and Wolfshtein, M., Heat and Mass Transfer in Recirculating Flows, Academic Press, 1969.

9. Spalding, D. B., Gosman, A. D., and Pun, W. M., The Prediction of Two-Dimensional Flows, Short Course, Pennsylvania State University, August 1972.

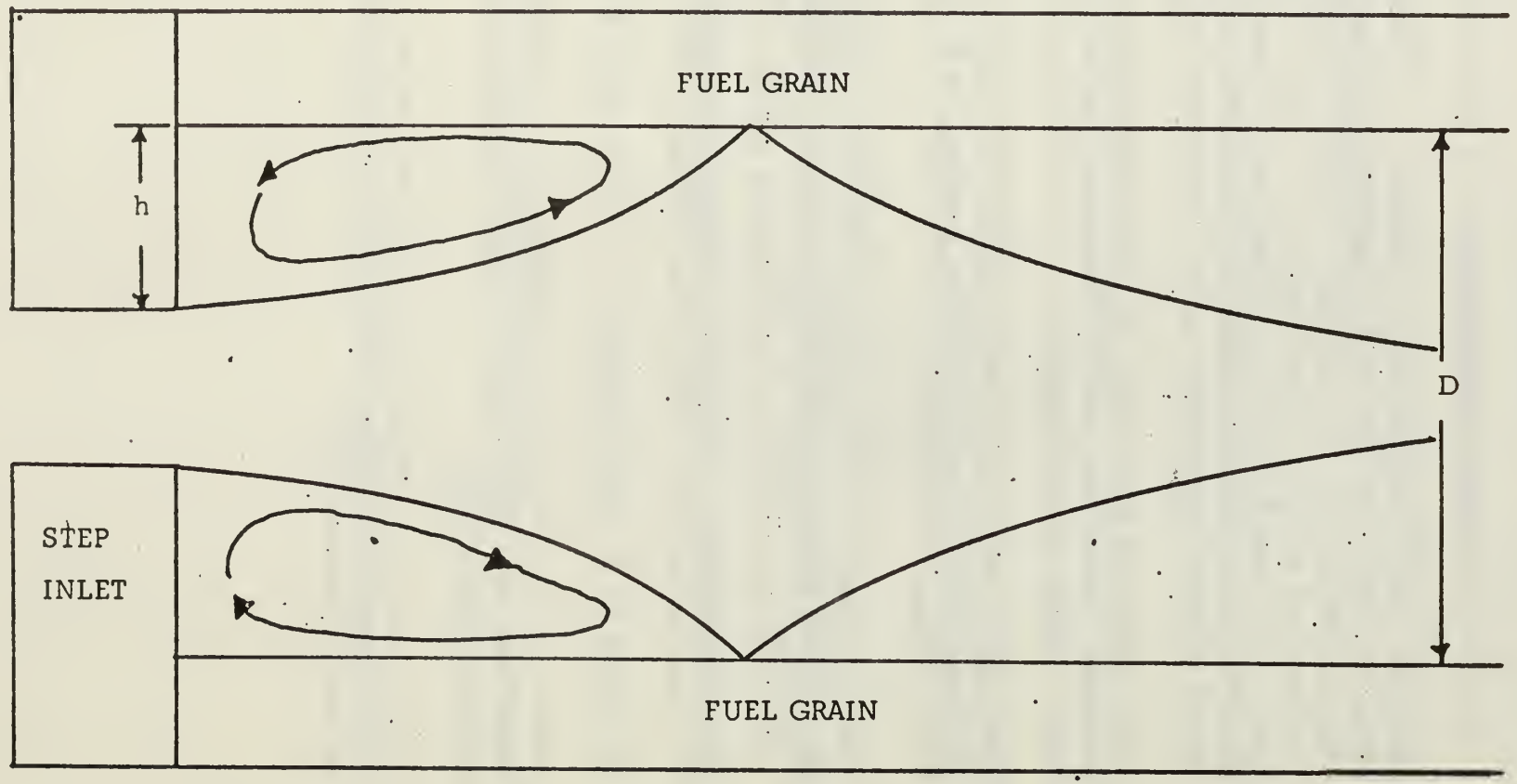

Figure 1. Combustion Mechanisms

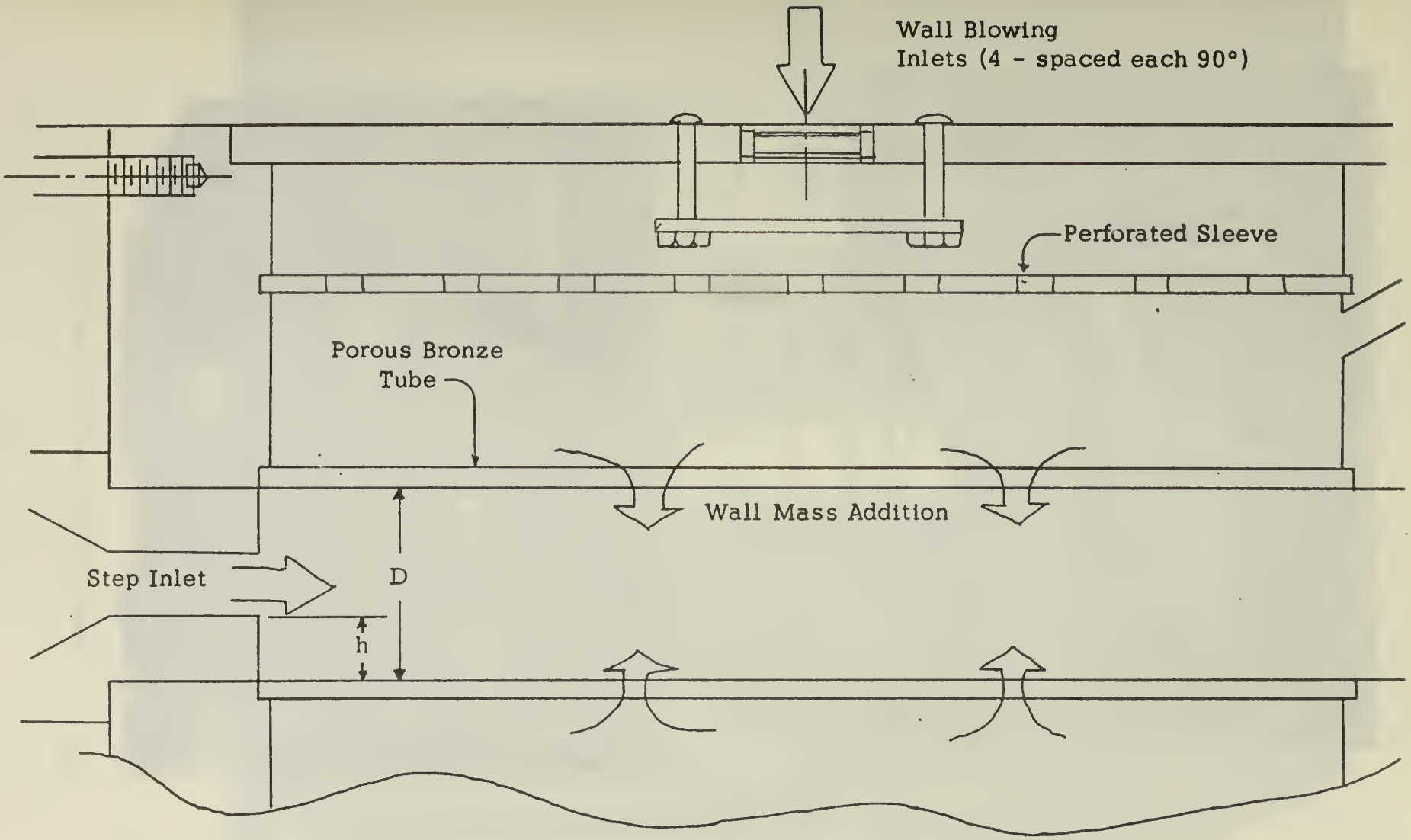

Figure 2 Schematic of ramjet model

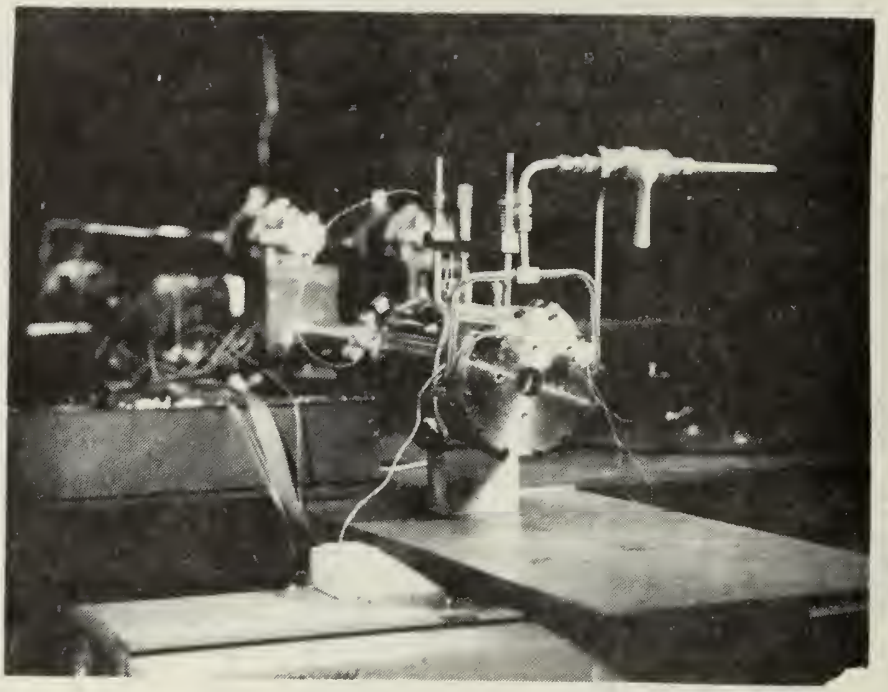

Figure 3. Ramjet Model Installed in Test Cell

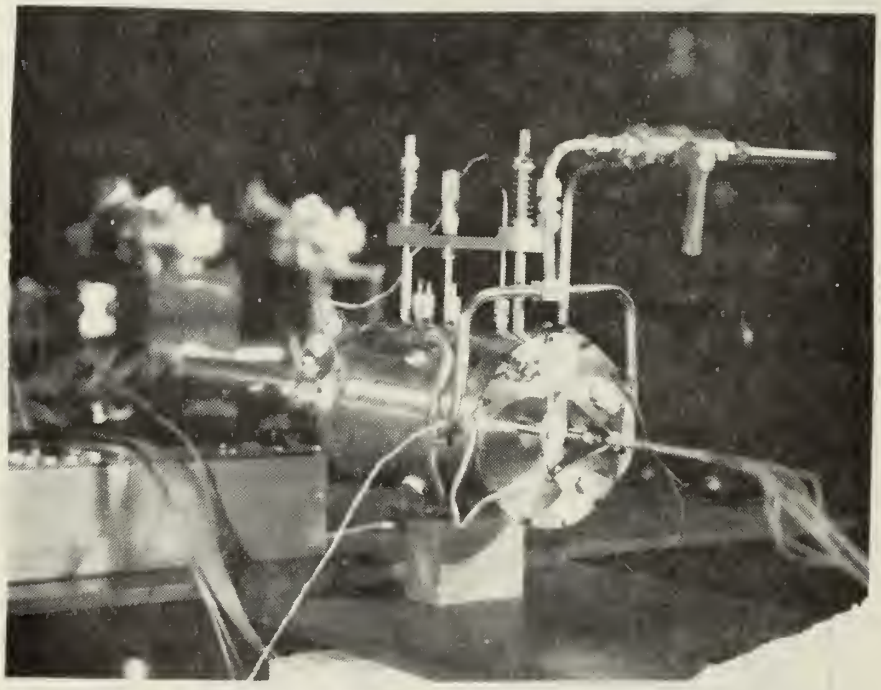

Figure 4. Ramjet Model with Pressure Probe Installed

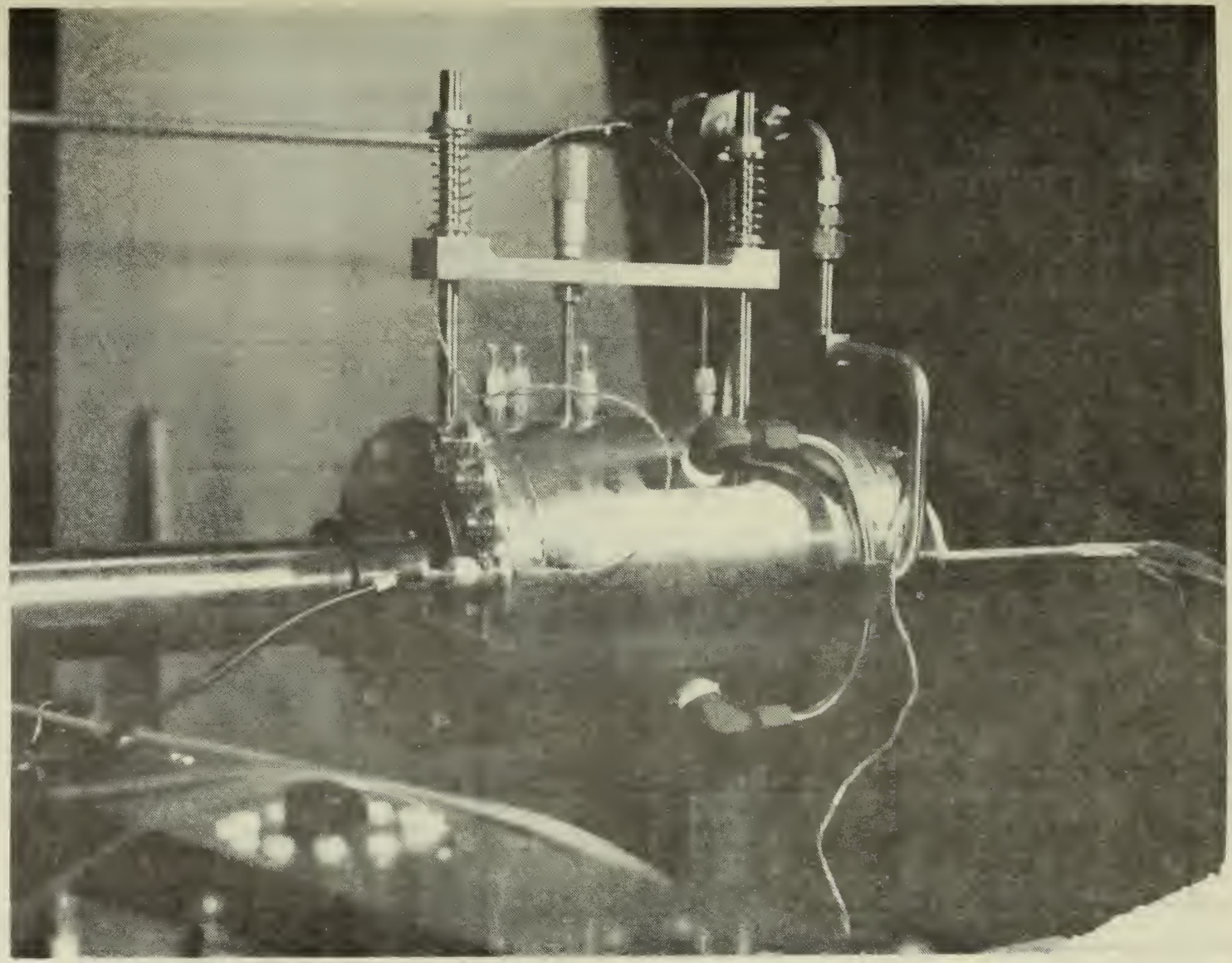

Figure 5. Detail of Hot Wire Traverse Apparatus

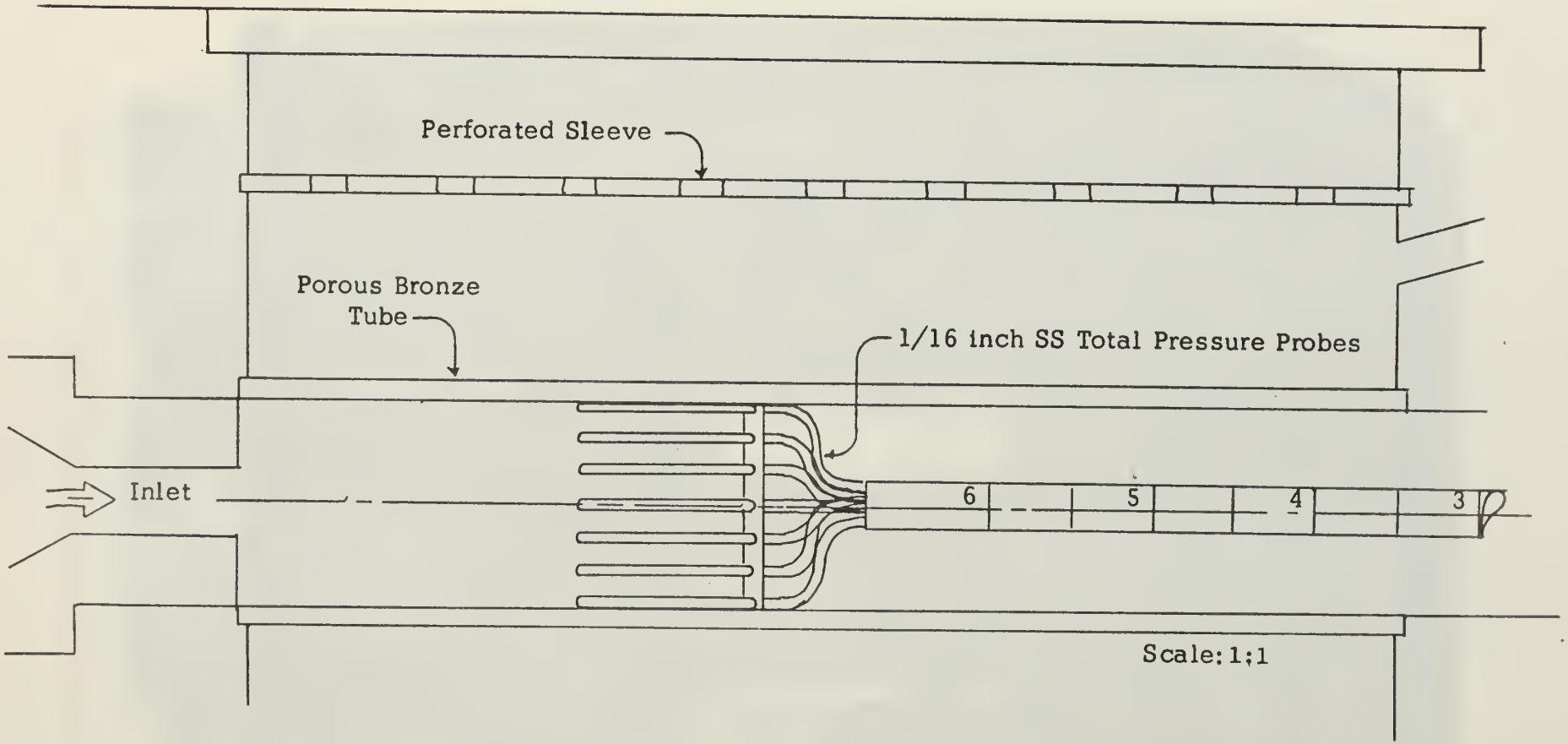

Figure 6. Total Pressure Rake - Installed

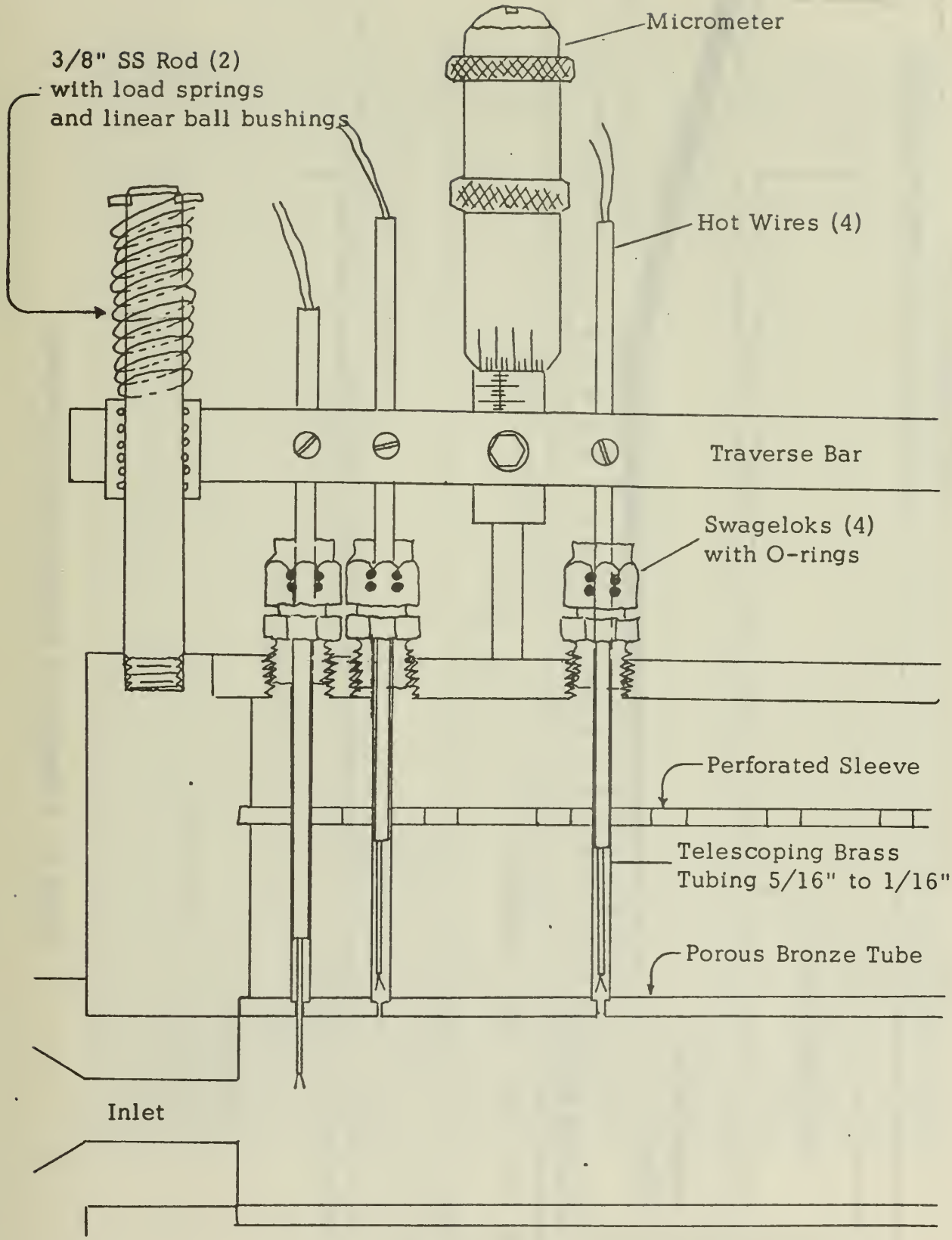

Figure 7. Schematic of Hot Wire Installation and Traverse

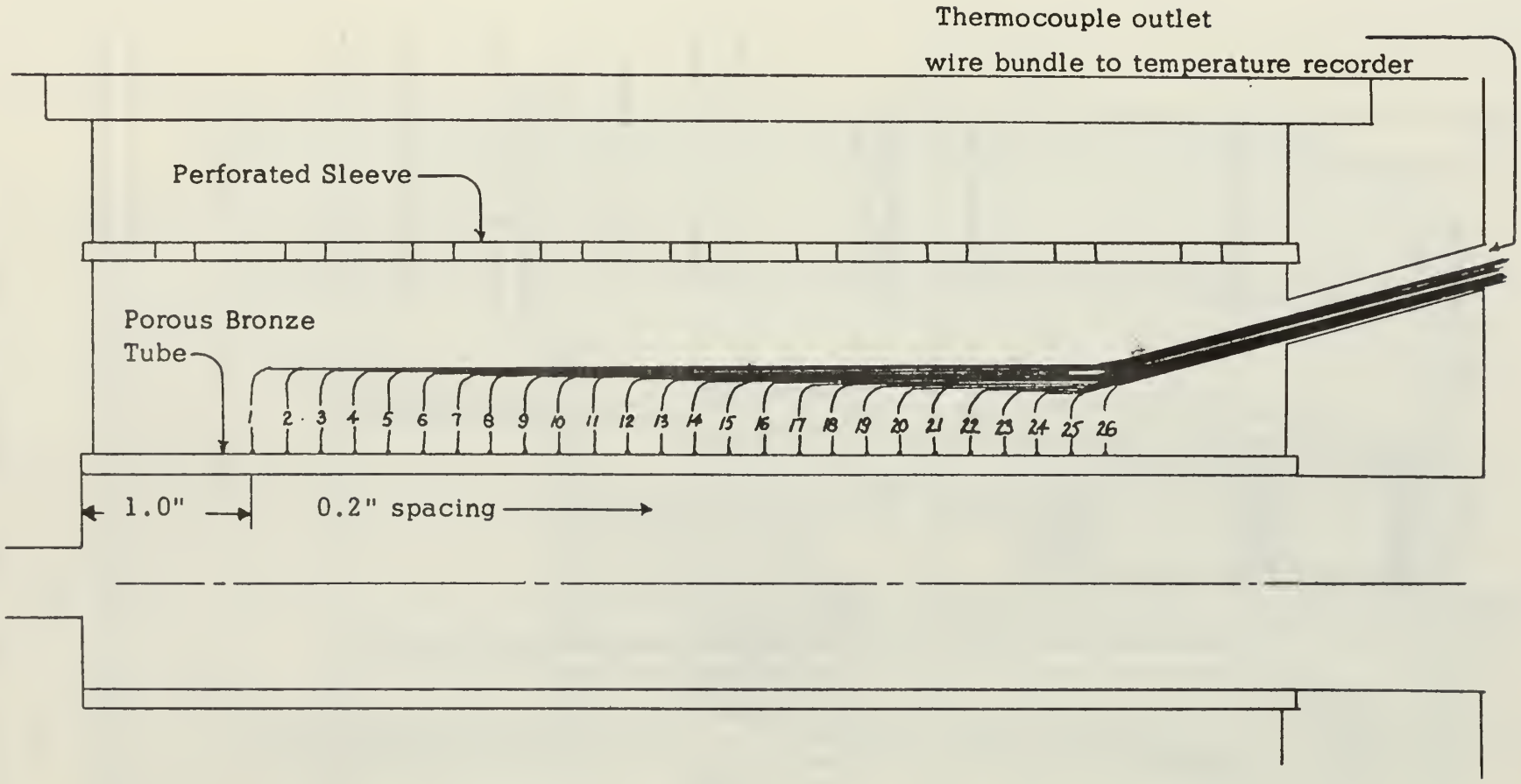

Figure 8. Schematic of Thermocouple Connections

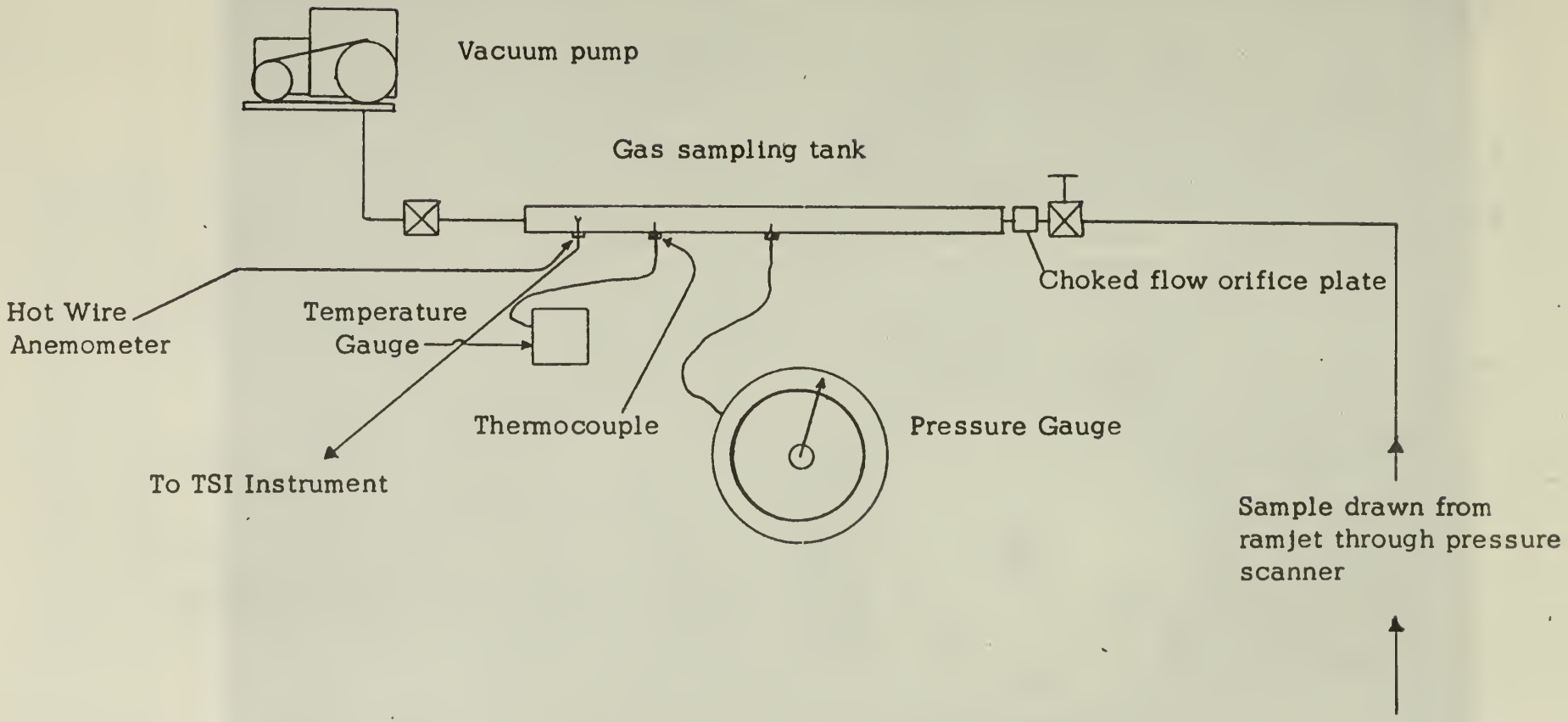

Figure 9. Schematic of Mass Fraction Analysis Apparatus

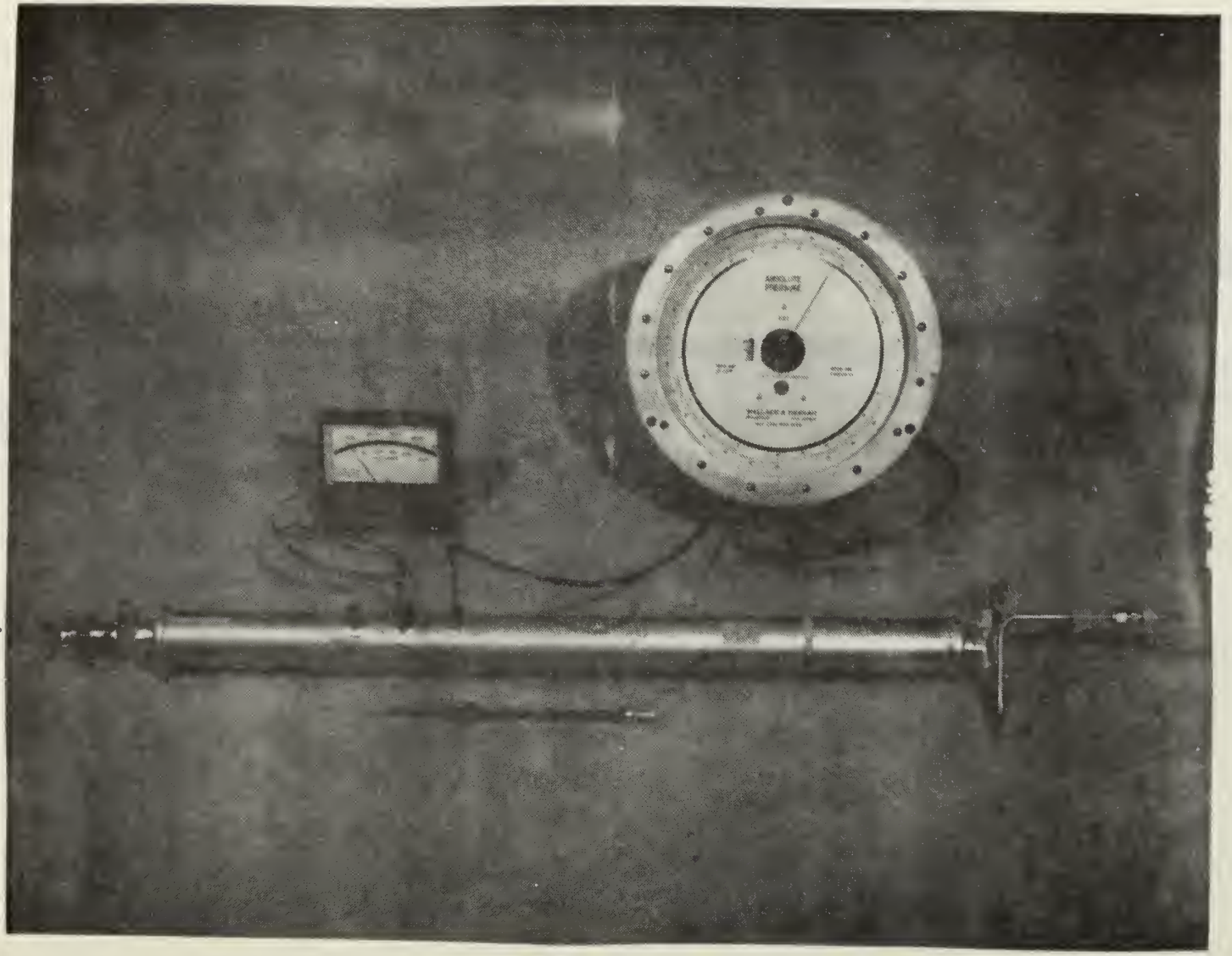

Figure 10. Mass Fraction Analysis Apparatus

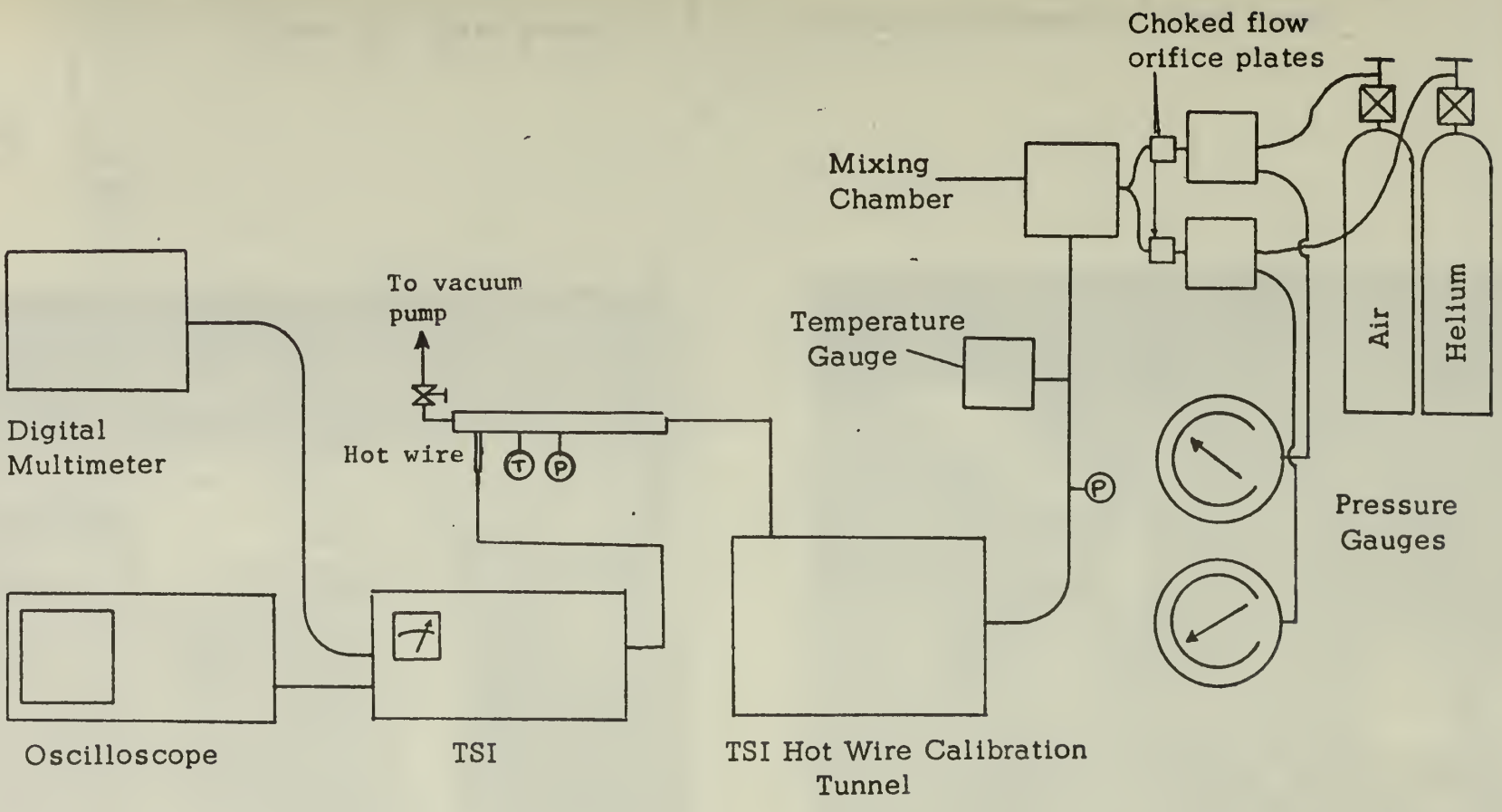

Figure 11. Schematic of Mass Fraction Hot Wire Calibration Apparatus

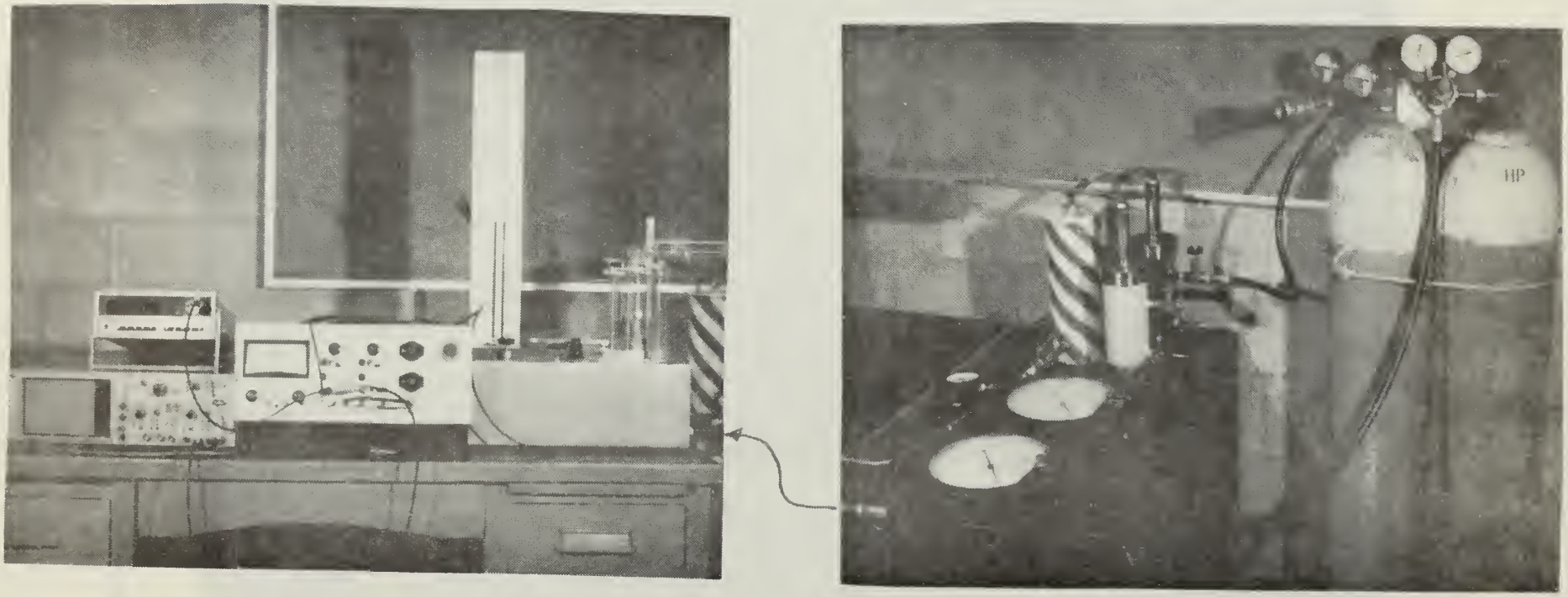

Figure 12. Mass Fraction Hot Wire Calibration Apparatus

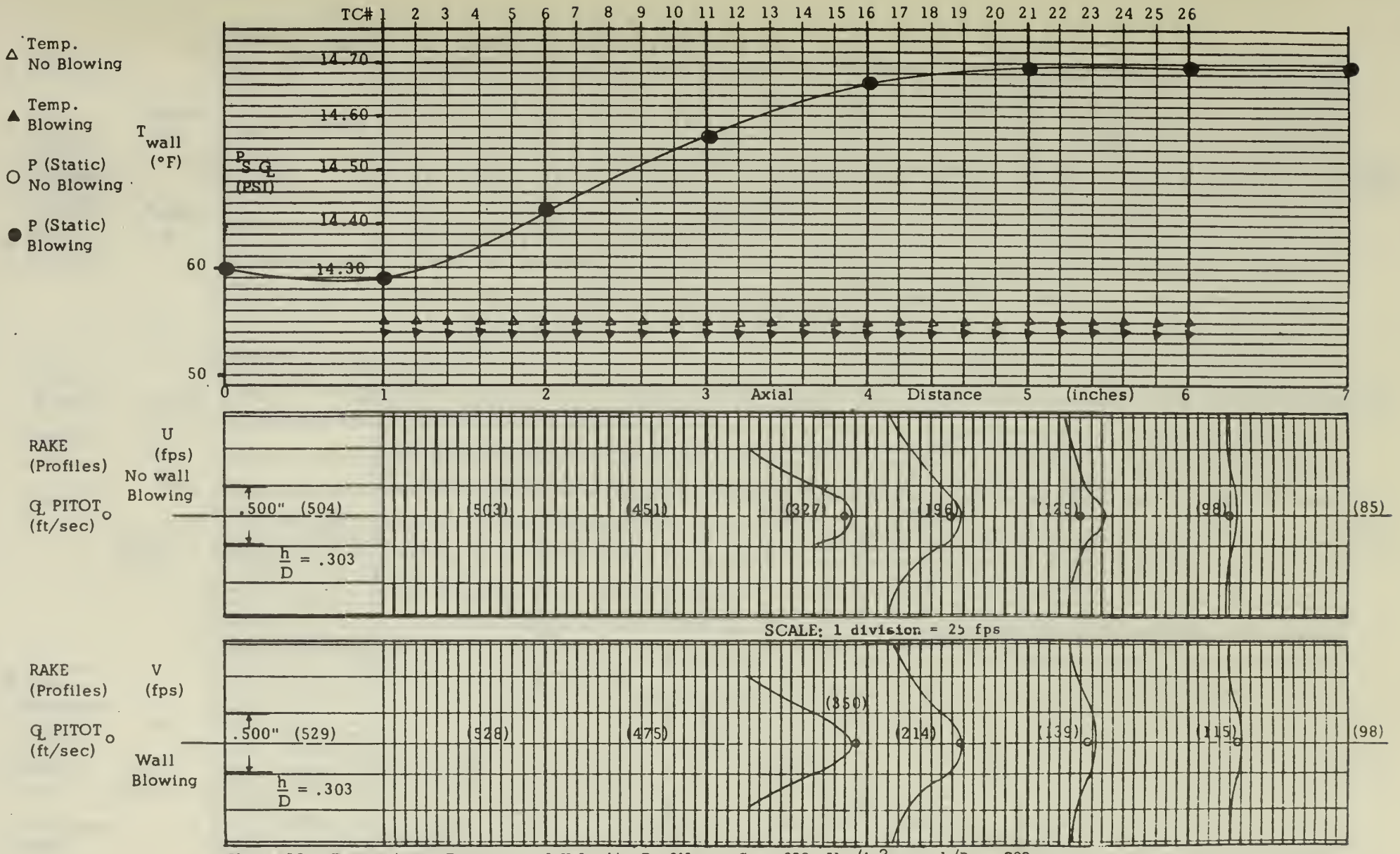

Figure 13. Temperature, Pressure and Velocity Profiles, G = .039 lb_m/in^2-sec, h/D = .303

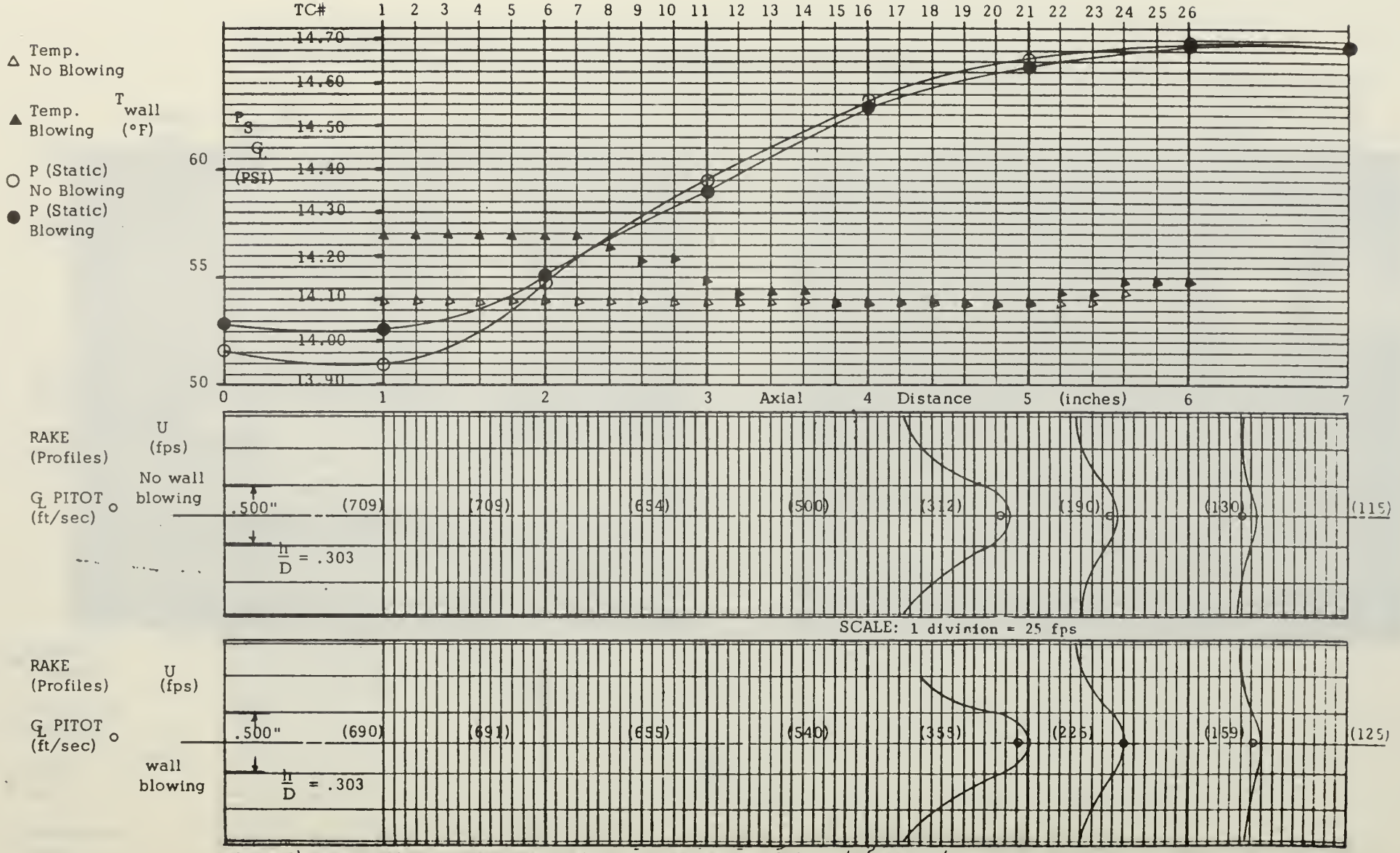

Figure 14. Temperature, Pressure and Velocity Profiles, $\bar{G} = .055$ lb_m/in^2-sec, h/D = .303

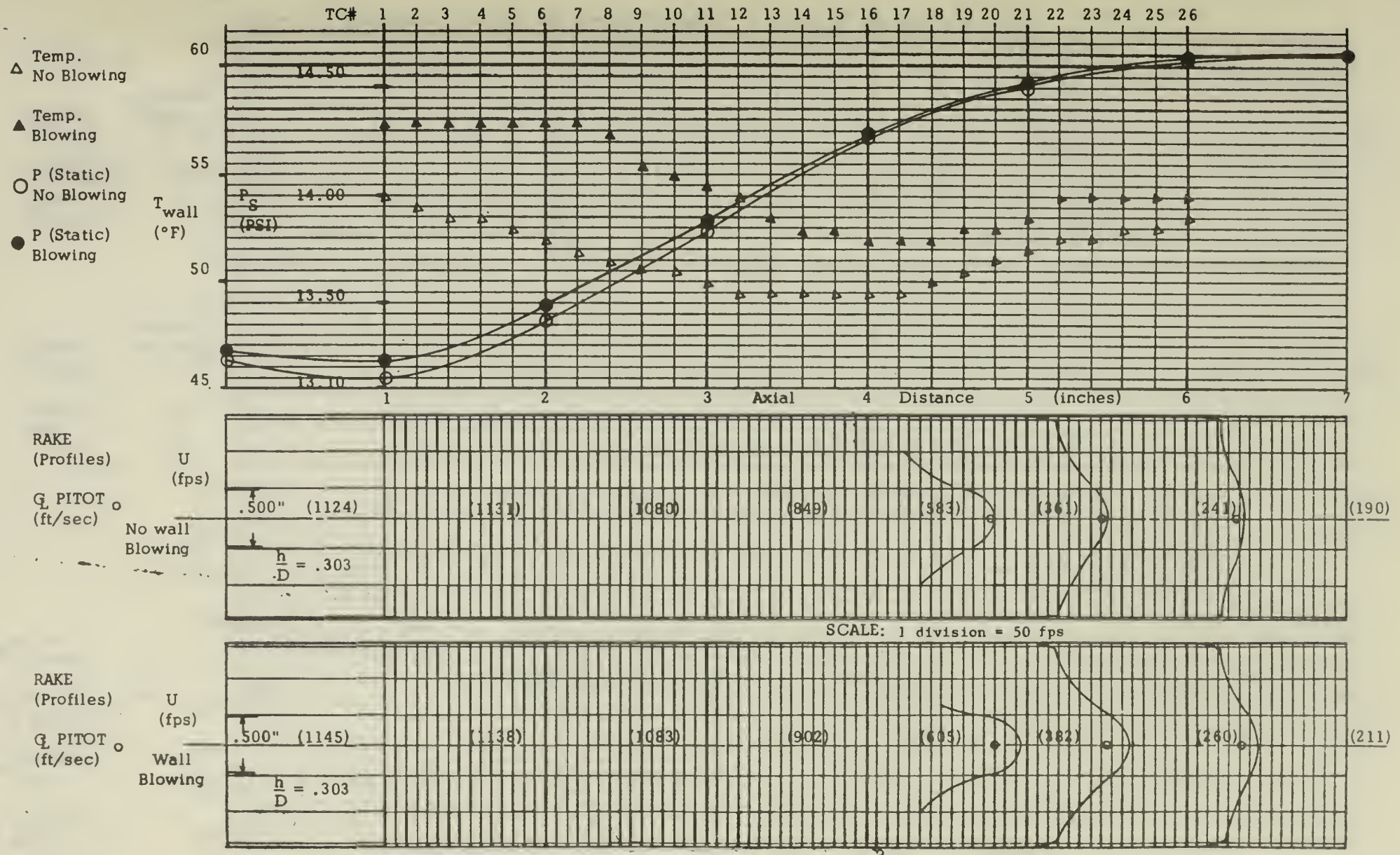

Figure 15. Temperature, Pressure and Velocity Profiles, G = .079 lb_m/in^2-sec, h/D = .303

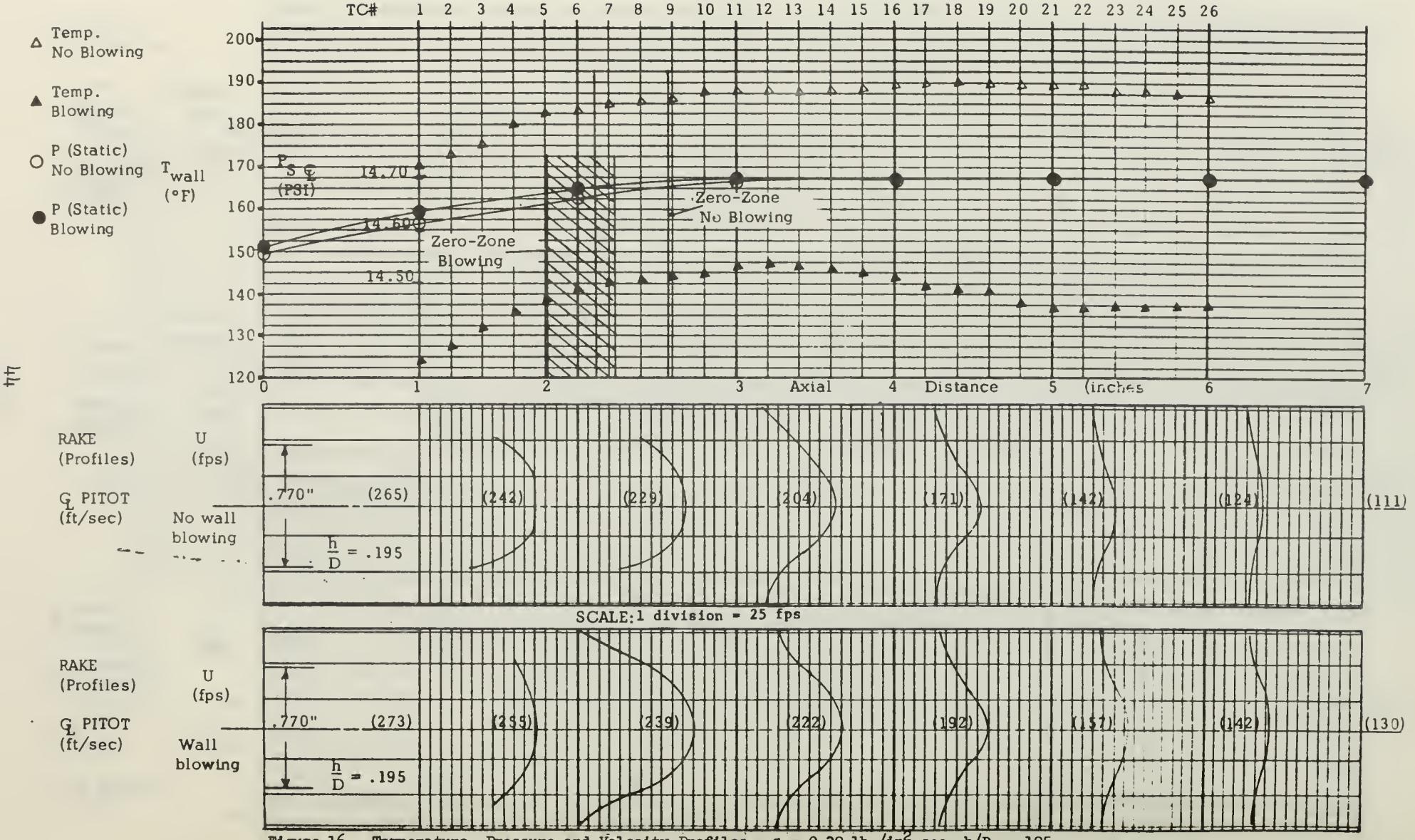

Figure 16. Temperature, Pressure and Velocity Profiles, $G = 0.39\ lb_m/in^2\text{-sec}$, $h/D = .195$

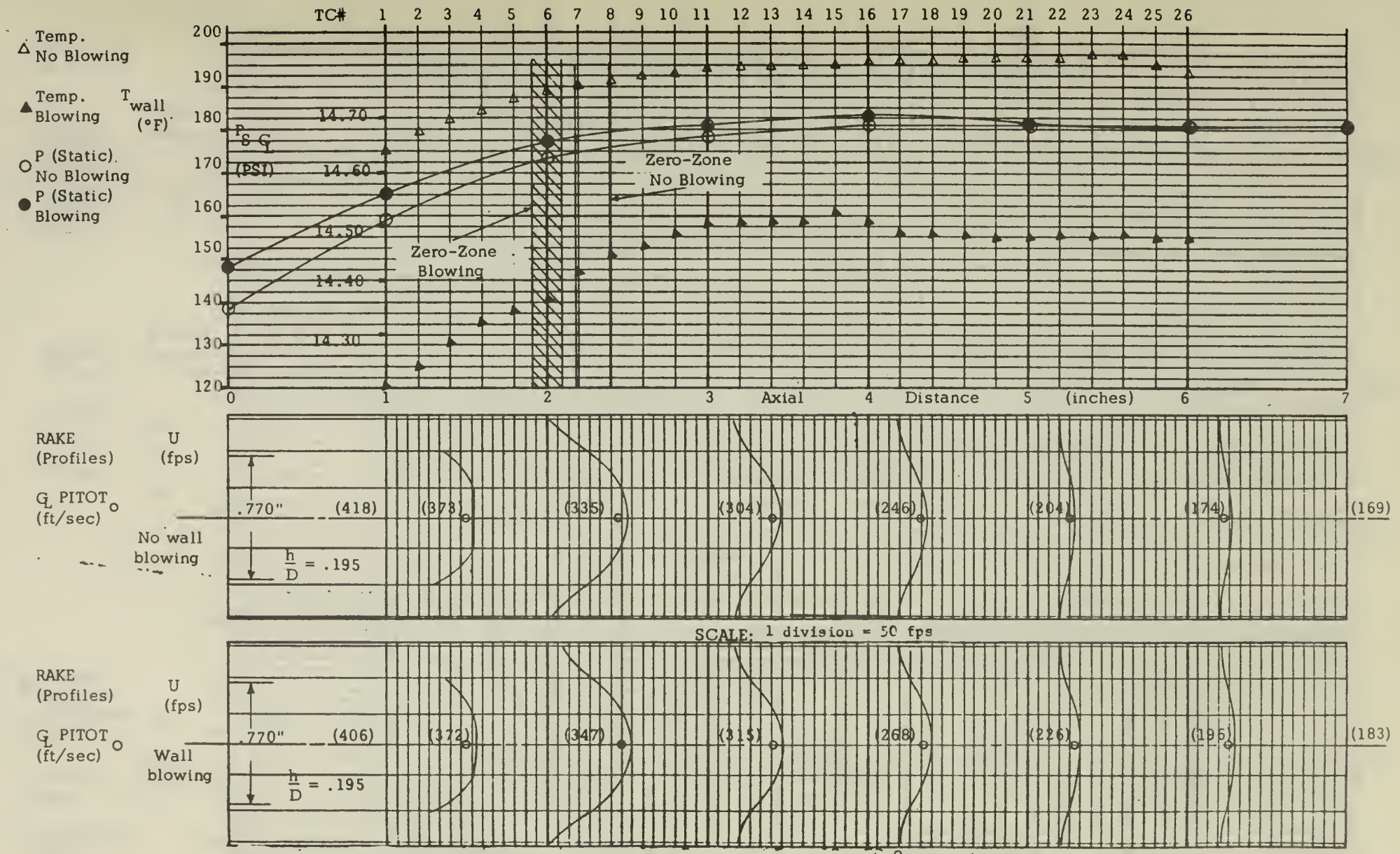

Figure 17. Temperature, Pressure and Velocity Profiles, G = .055 lb_m/in^2-sec, h/D = .195

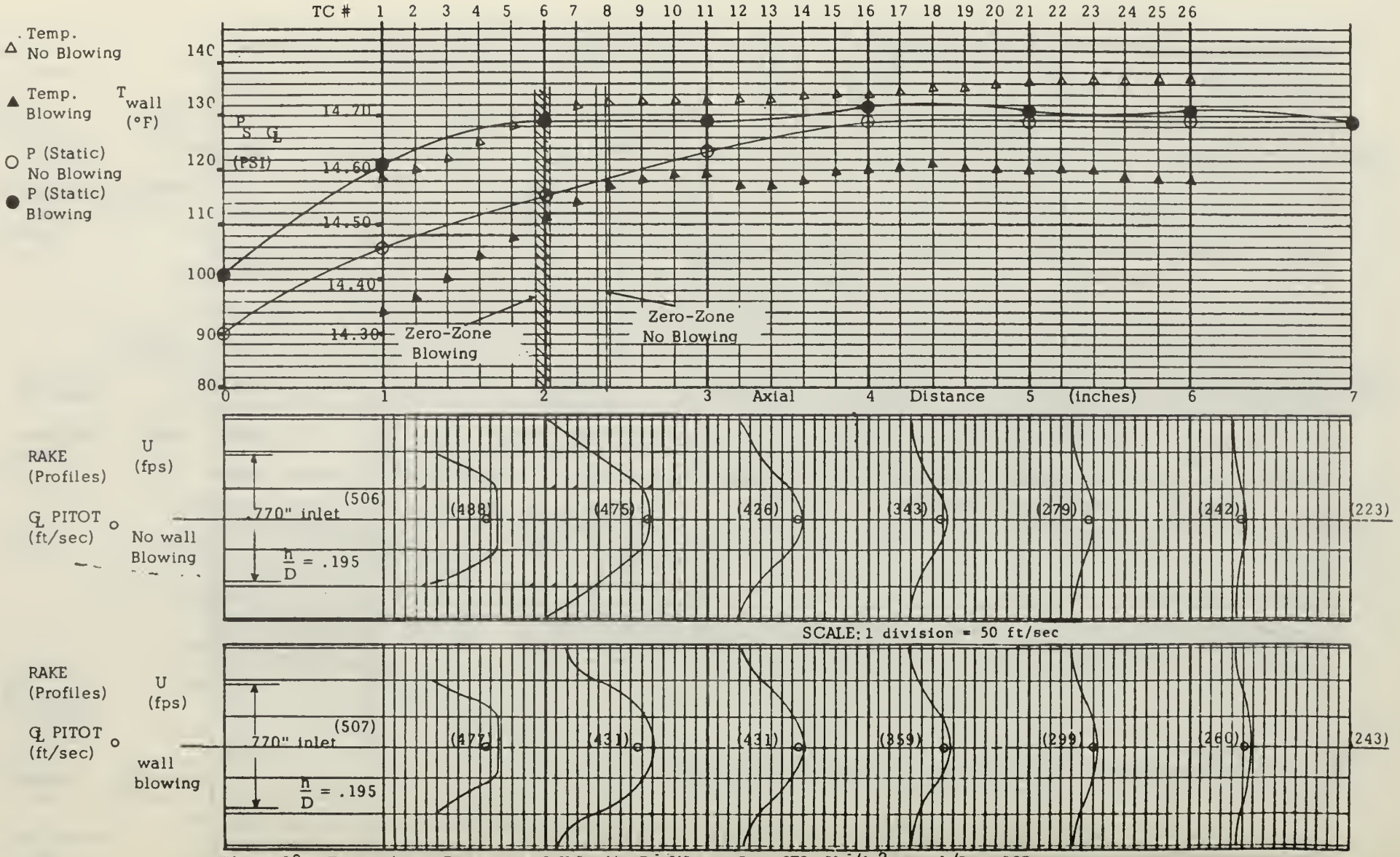

Figure 18. Temperature, Pressure and Velocity Profiles. G = .079 lb_m/in^2-sec, h/D = .195

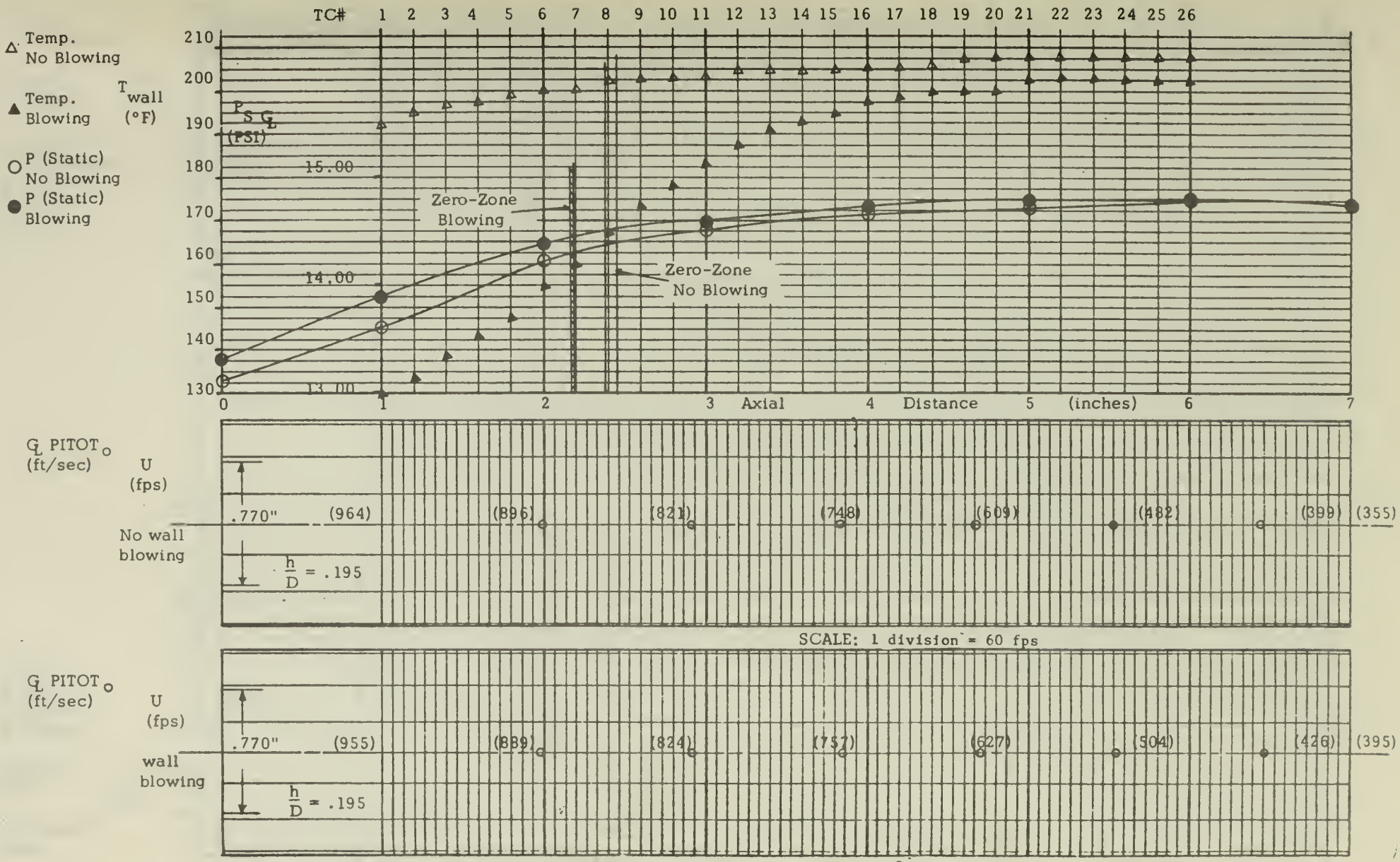

Figure 19. Temperature, Pressure and Velocity Profiles, G = .118 lb_m/in^2-sec, h/D = .195

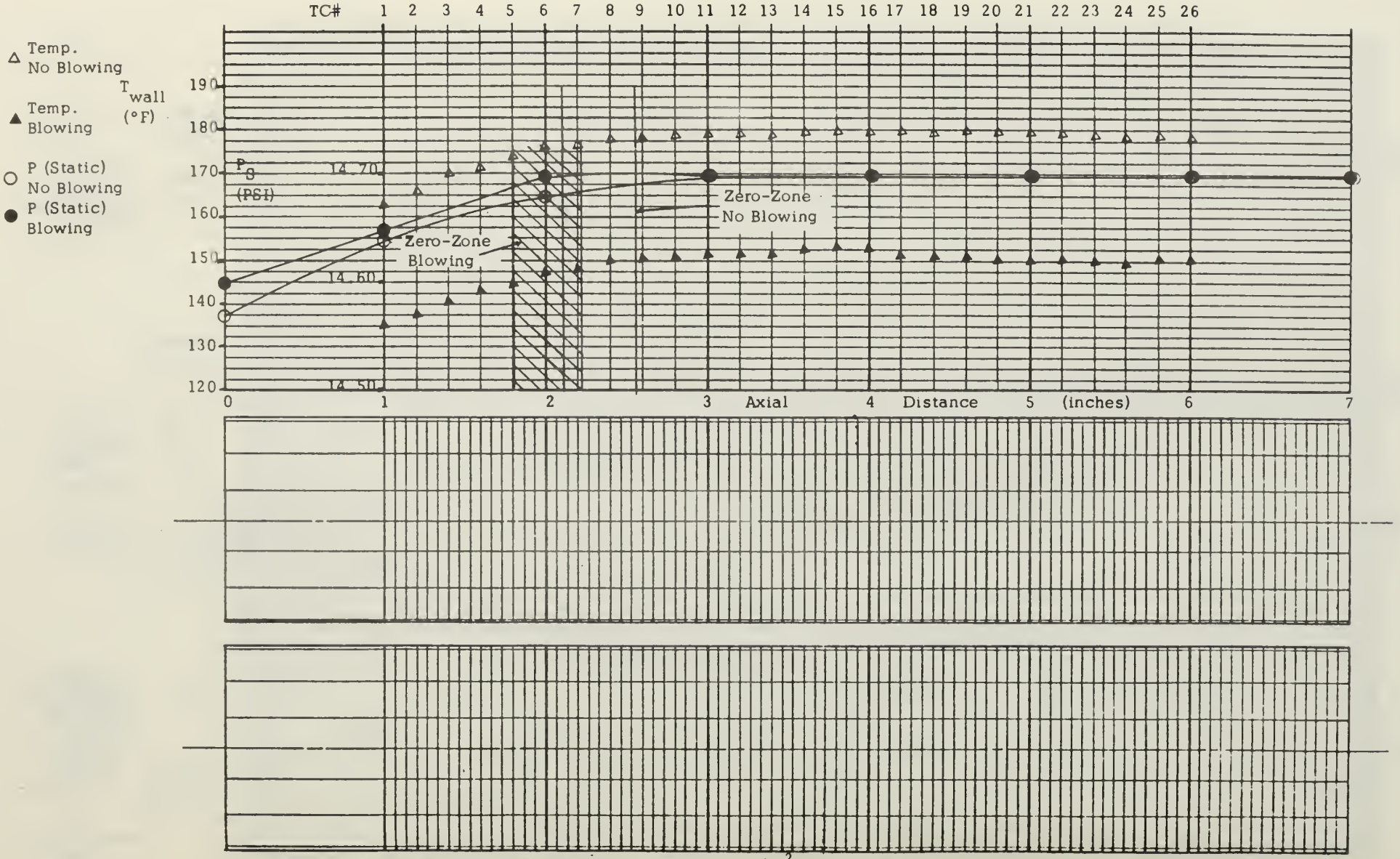

Figure 20. Reattachment Point Measurements, G = .039 lb_m/in^2-sec, h/D = .105

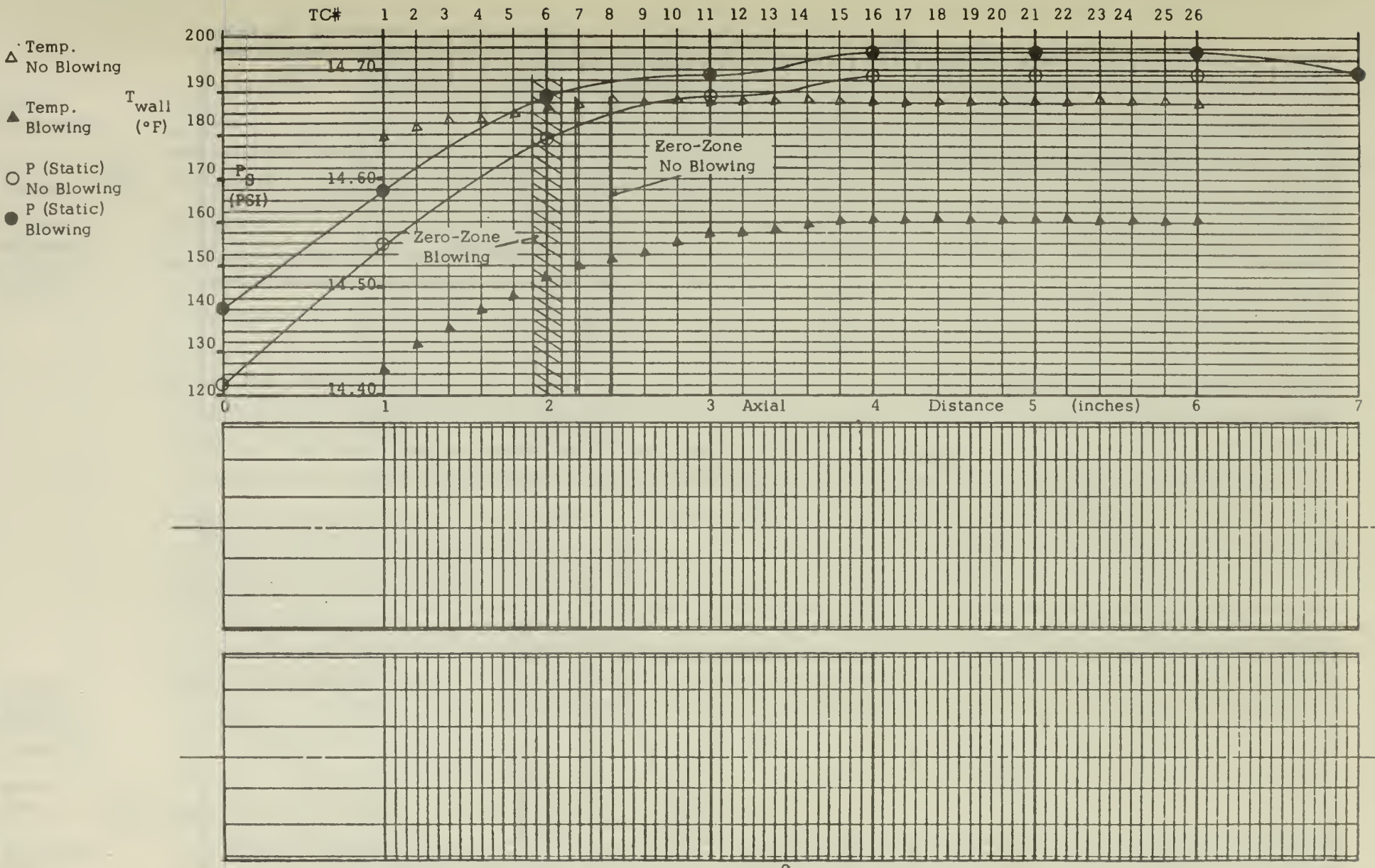

Figure 21. Reattachment Point Measurements, G = .055 lb_m/in^2-sec, h/D = .195

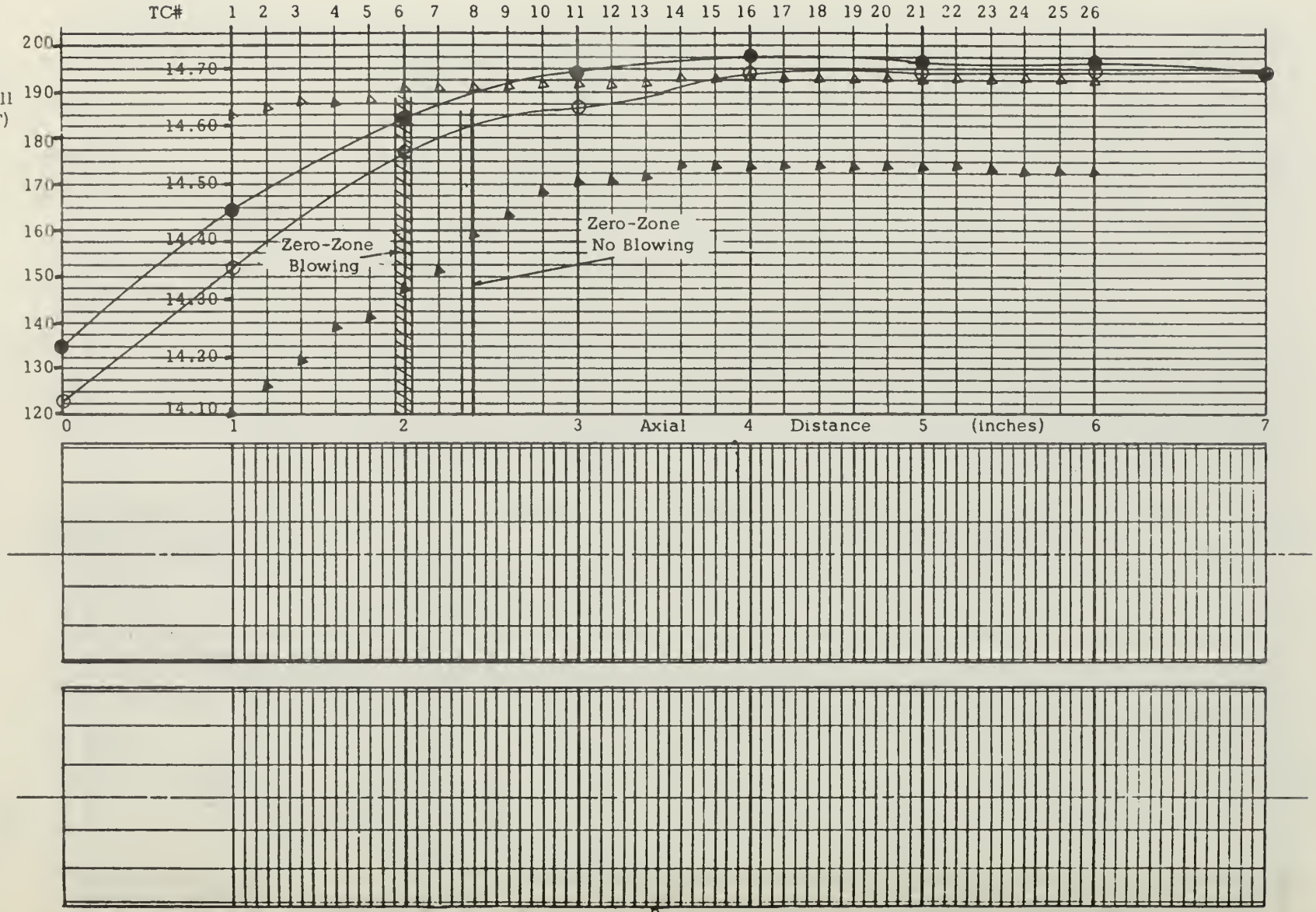

Figure 22. Reattachment Point Measurements, G = .079 lb_m/in^2-sec, h/D = .195

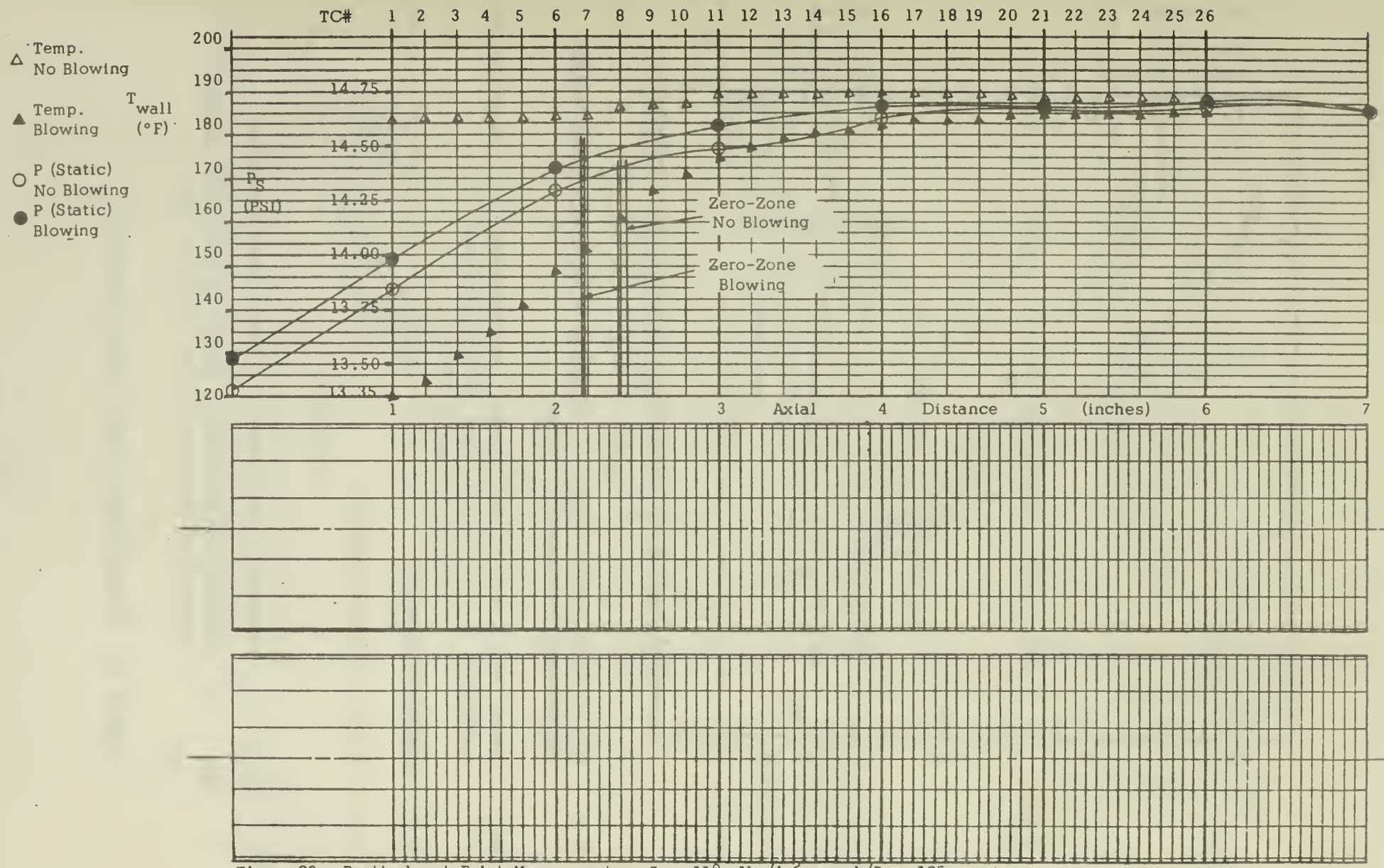

Figure 23. Reattachment Point Measurements, G = .118 lb_m/in^2-sec, h/D = .195

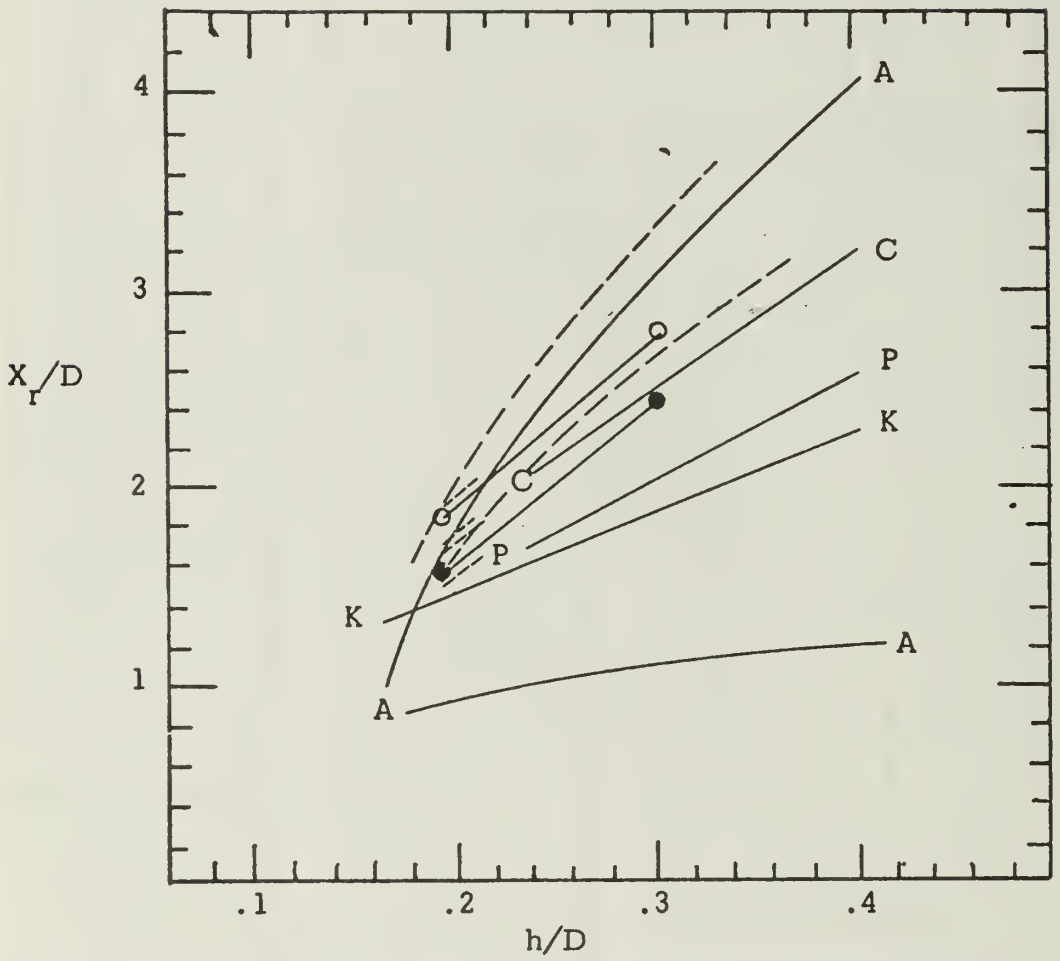

K-K Krall and Sparrow - based on location of maximum heat transfer coefficient (axisymmetric flow)

A-A Abbott and Kline - note different reattachment point locations for each side of 2-D channel and spread-out zone

P-P PISTEP II results

C-C Boaz and Netzer results

Present Investigation - no wall mass addition

Present Investigation - with 10% wall mass addition showing spread-out region at h/D = .195

Figure 24. Reattachment Point Data Comparison

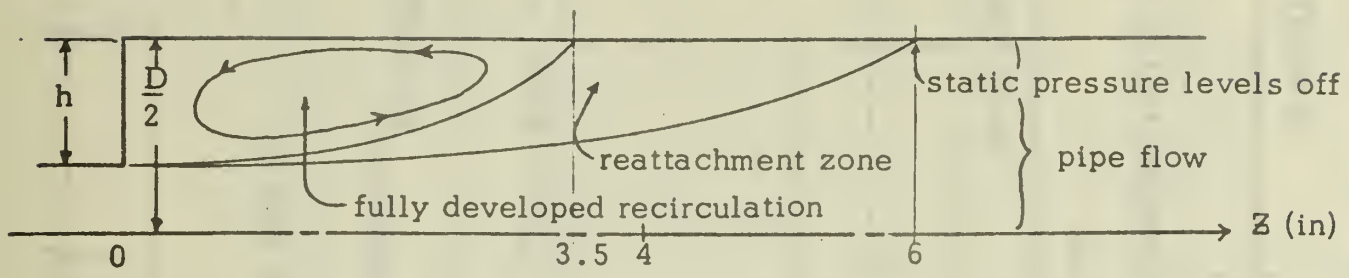

Figure 25. Typical Reattachment Zone - Large Step

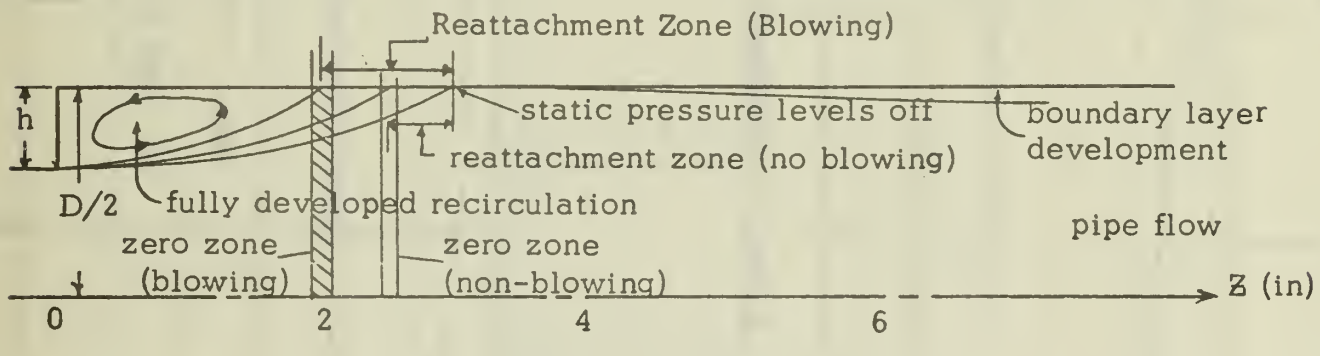

Figure 26. Typical Reattachment Zone - Small Step

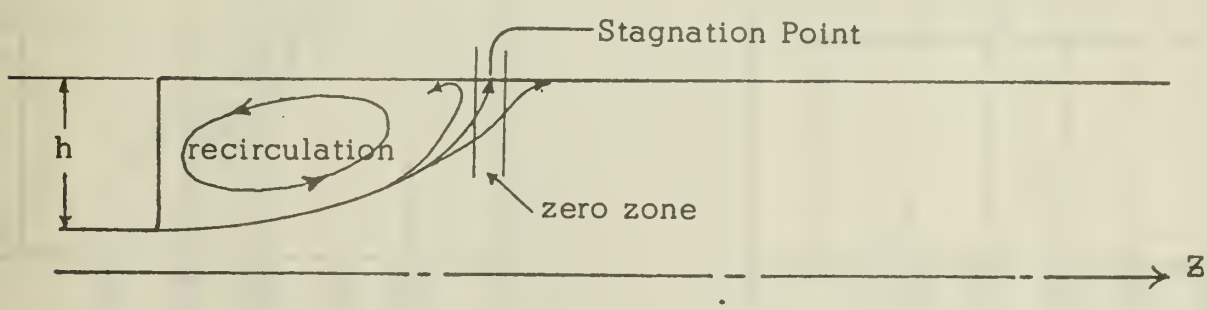

Figure 27. "Zero Zone" Leading Edge of Flow Reattachment

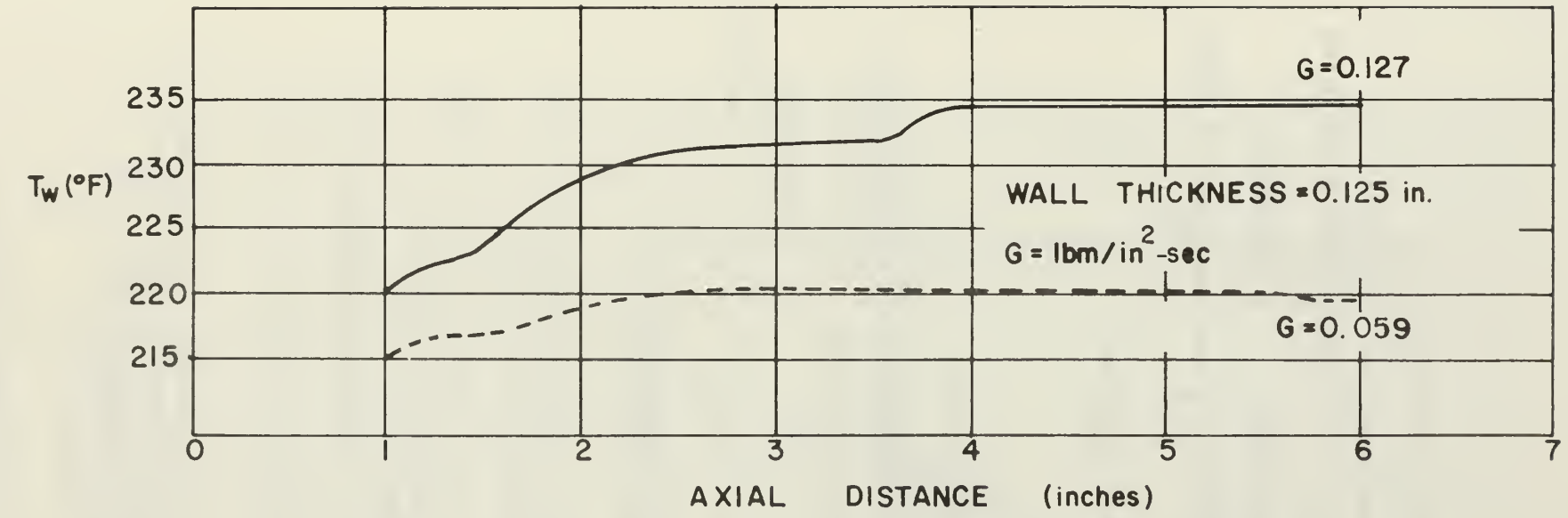

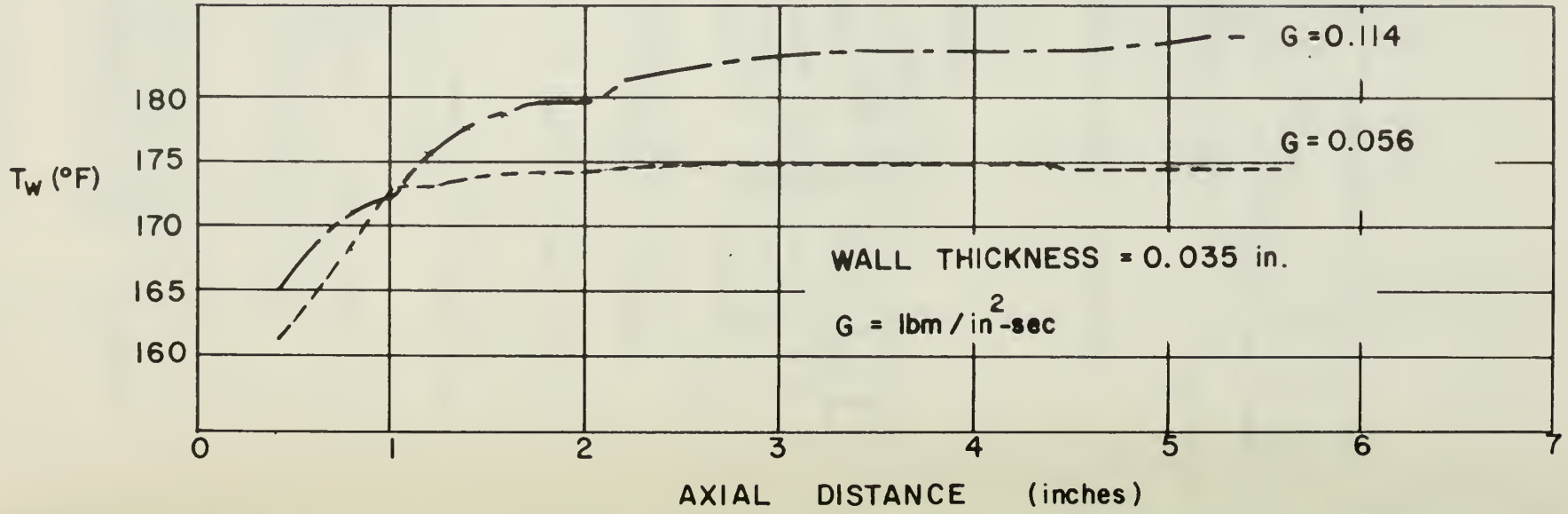

Figure 28. WALL TEMPERATURE PROFILES, SOLID WALL, h/D = 0.195

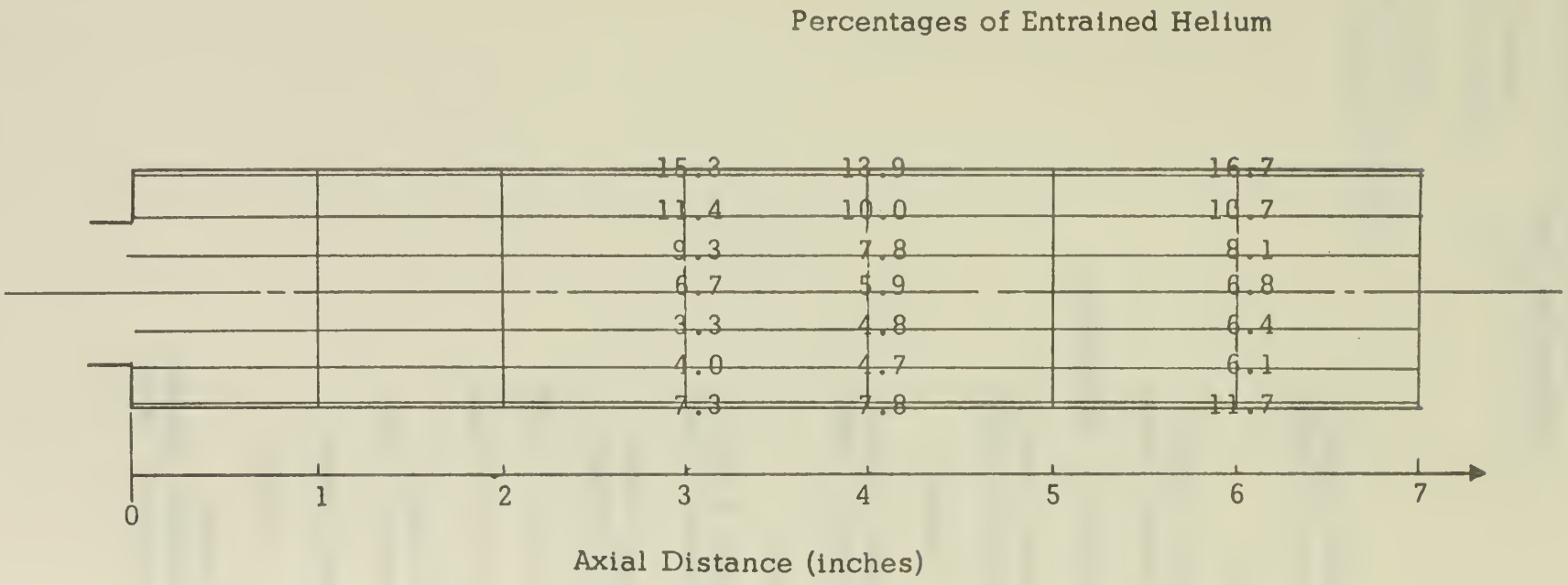

Figure 29. Mass Fraction Distribution

DISTRIBUTION LIST

		No. of copies
1.	Library Code 0212 Naval Postgraduate School Monterey, California 93940	2
2.	Dean of Research Code 023 Naval Postgraduate School Monterey, California 93940	2
3.	Chairman, Department of Aeronautics Code 57 Naval Postgraduate School Monterey, California 93940	1
4.	Professor D. W. Netzer Code 57 Naval Postgraduate School Monterey, California 93940	10
5.	LCDR J. T. Phaneuf Code 31 Naval Postgraduate School Monterey, California 93940	2
6.	United Technology Center Attn: Technical Library P.O. Box 358 Sunnyvale, California 94088	1
7.	Defense Documentation Center Attn: DDC-TCA Cameron Station, Bldg. 5 Alexandria, Virginia 22314	12
8.	Naval Air Systems Command Attn: AIR-330 Washington, D.C. 20360	2
9.	Naval Weapons Center Attn: Code 753-Tech. Library China Lake, California 93555	3

10. Chemical Propulsion Information Agency 2
APL-JHU
8621 Georgia Avenue
Silver Spring, Maryland 20910

11. Naval Weapons Center 2
Attn: D. Bullat, Code 4576
China Lake, California 93555